ACS APPLIED MATERIALS & INTERFACES

Research Article

www.acsami.org

Origin of Superlubricity in a-C:H:Si Films: A Relation to Film Bonding Structure and Environmental Molecular Characteristic

Xinchun Chen,* Takahisa Kato, and Masataka Nosaka

Department of Mechanical Engineering, The University of Tokyo, 113-8656 Tokyo, Japan

ABSTRACT: Superlubricity of Si-containing hydrogenated amorphous carbon (a-C:H:Si) films has been systematically investigated in relation to the film bonding structure and the environmental atmosphere. Structural diversity induced by hydrogen incorporation (i.e., 17.3−36.7 at. % H), namely sp^2-bonded a-C, diamond-like or polymer-like, and tribointeractions activated by the participation of environmental gaseous molecules mainly determine the frictional behaviors of a-C:H:Si films. A suitable control of hydrogen content in the film (i.e., the inherent hydrogen coverage) is obligate to obtain durable superlubricity in a distinct gaseous atmosphere such as dry N_2, reactive H_2 or humid air. Rapid buildup of running-in-induced antifriction tribolayers at the contact interface, which is more feasible in self-mated sliding, is crucial for achieving a superlubric state. Superior tribological performances have been observed for the polymer-like a-C:H:Si (31.9 at. % H) film, as this hydrogen-rich sample can exhibit superlow friction in various atmospheres including dry inert N_2 ($\mu \sim 0.001$), Ar ($\mu \sim 0.012$), reactive H_2 ($\mu \sim 0.003$) and humid air ($\mu \sim 0.004$), and can maintain ultralow friction in corrosive O_2 ($\mu \sim 0.084$). Hydrogen is highlighted for its decisive role in obtaining superlow friction. The occurrence of superlubricity in a-C:H:Si films is generally attributed to a synergistic effect of phase transformation, surface passivation and shear localization, for instance, the near-frictionless state occurred in dry N_2. The contribution of each mechanism to the friction reduction depends on the specific intrafilm and interfilm interactions along with the atmospheric effects. These antifriction a-C:H:Si films are promising for industrial applications as lubricants.

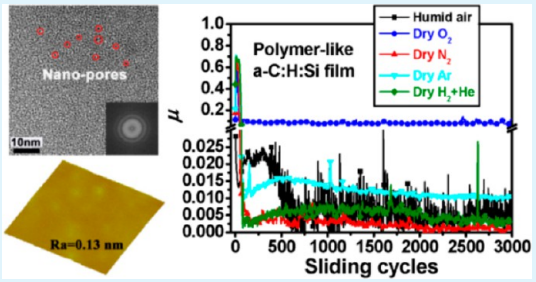

KEYWORDS: *superlubricity, a-C:H:Si, hydrogen, film structure, environmental atmosphere, polymer-like*

1. INTRODUCTION

Friction and wear is one of the major causes for energy dissipation and equipment failure during industrial activities.[1] The realization of a friction-free state is therefore of high significance both from the basic scientific perspective of tribology and in view of the potential industrial applications it carries. In general, the sliding state with low friction coefficient μ can be divided into two levels: (i) ultralow friction, where $0.01 < \mu < 0.1$ and (ii) superlow friction, where $\mu < 0.01$.[2] The latter one is defined as "superlubricity", originally proposed by Hirano and Shinjo in 1990, describing a theoretical sliding state where friction or resistance to sliding nearly vanishes.[3] The predictive existence of such a near-frictionless state stimulates numerous theoretical and experimental studies on superlubricity.[4−13] In the past decades, some carbon-based films such as graphite,[6,14] carbon nitride (CN_x),[15] highly hydrogenated amorphous carbon (a-C:H),[8−11] tetrahedral amorphous carbon (ta-C),[16] metal-doped nanocomposite (TiC/a-C:H),[17] fullerene-like carbon (i.e., FL-CN_x, FL-C:H),[18,19] ultrananocrystalline diamond (UNCD)[7,12,20,21] and diamond nanowire (DNW)[22,23] have been designed to explore the possibilities for achieving ultralow or even superlow friction.

Until now, two well-known mechanisms have been proposed to disclose the friction-reducing behaviors in these carbon films. One is shear-induced carbon phase transformation such as sp^3-C to sp^2-C rehybridization at the sliding interface,[24−27] where the sp^2-C phase is thought to be a softer and low-shear strength phase. For instance, the possible formation of a graphitic tribolayer on the contact surface has been studied by various characterization methods in diamond-like carbon (DLC) films during sliding.[26,27] The other prevailing mechanism is surface passivation of dangling bonds at the sliding interface by passivating species such as −H, −OH or water molecules.[8−12,20,21,28] For example, the extremely low friction coefficients down to 0.001 of highly hydrogenated a-C:H film are mainly attributed to the surface chemical inertness by H-passivation of carbon dangling σ bonds and the resulting little adhesive force exerted at the sliding interface.[8−11,28] A similar friction-reduction mechanism has also been found for lubricity of ta-C by glycerol[16] and UNCD[12,20,21] or O_2-plasma-treated DNW[22,23] by H_2O molecules. More recently, a shear localization mechanism has been postulated to explain the lubricity in a-C.[29,30] Shear localization is characteristic of phase transformation (i.e., sp^3-to-sp^2), bond reorientation and structural ordering preferentially in a localized region, namely the tribolayer, resulting in shear weakening. Superlow friction is only feasible under the conditions of high phase transformation (i.e., sp^2 fraction more than 80%) and high shear localization

Received: February 8, 2014
Accepted: August 6, 2014
Published: August 6, 2014

Table 1. Overview of Properties of a-C:H:Si Films[a]

bias voltage (kV)	composition (at. %) H	C	Si	O	N	*Ra* (nm)	*H* (GPa)	*E* (GPa)	σ (GPa)	*x*
0.25	36.7	52.5	9.3	1.2	0.3	0.08	13.8	123.9	0.78	0.059
0.5	31.9	57.2	9.3	1.2	0.4	0.13	16.2	155.7	1.04	0.031
1.0	25.8	61.2	9.2	2.7	1.1	0.17	17.9	175.7	1.41	0.017
1.5	23.2	64.8	9.1	2.1	0.8	0.09	17	176.1	1.12	0.021
2.0	20.8	68.1	8.9	1.7	0.5	0.11	17.3	178.6	1.0	0.015
2.5	20.5	66.6	9.6	3.0	0.3	0.1	15.8	166	0.77	0.007
3.0	18.2	68.8	9.7	2.7	0.6	0.09	15.2	164.3	0.86	0.022
3.5	17.3	70.1	9.9	2.0	0.7	0.09	14.9	150.2	0.84	0.006

[a] As reported in ref 32, including composition, roughness *Ra*, hardness *H*, elastic modulus *E*, residual stress σ and viscoplastic exponent *x*, as a function of bias voltage.

(i.e., orientations of most covalent bonds parallel to the sliding direction) in the very thin localized layer around the sliding interface.[30] Shear localization is a supplement to the lubrication mechanism of a-C because, on one hand, simple phase transformation cannot guarantee superlow friction, and on the other hand, passivating species are not able to totally shield dangling bonds, especially in the sliding cases where dissociation and removal of surface terminations occurs.

Recently, we have reported the realization of superlubricity in energetic ion grown a-C:H:Si films in humid air.[31] As described in the previous work, a series of a-C:H:Si films containing different Si contents were synthesized using a tetramethylsilane (TMS) and toluene (C_7H_8) gas mixture in an ionization system under a pulsed bias voltage of 2 kV. The results indicate that superlow friction is feasible in humid air for a-C:H:Si films by dissociative formation of hydrophilic Si−OH groups passivating on film surface along with the adsorbed boundary water layer under appropriate contact pressure when the Si content was optimized at ∼8.4 at. %.[31] In a following work,[32] we changed the applied bias voltage from 0.25 to 3.5 kV to obtain different hydrogen contents in the films because hydrogen is a key factor affecting the structural and frictional properties of a-C:H films, while keeping the Si content almost constant at ∼9−10 at. % by fixing the gas flow ratio of 1. It is shown that the bonding structure depending on ion energy evolves from chain-developed polymer-like to cross-linked diamond-like, and finally to sp^2-bonded a-C as the hydrogen content gradually decreases from 36.7 to 17.3 at. %.[32] Therefore, it is of high interest to further investigate the structural dependence of frictional behaviors of these a-C:H:Si films in different gaseous environments.

In this work, we provide a systematic study on the frictional behaviors of a-C:H:Si films depending on the film bonding structure (i.e., hydrogen content) and the environmental atmospheres including dry inert N_2, reactive H_2 and humid air. Special efforts were devoted to characterizing the polymer-like a-C:H:Si films in view of their superior antifriction performances compared to other structured films. The underlying lubrication mechanism is discussed from the perspective of each contribution of phase transformation, surface passivation and/or shear localization to the friction-reduction behaviors of a-C:H:Si films.

2. EXPERIMENTAL METHODS

The a-C:H:Si films with different hydrogen contents were prepared at a fixed gas flow ratio of TMS/C_7H_8 by varying the applied bias voltage from 0.25 to 3.5 kV in an ionization system. Relevant details on the growth conditions and structural investigations are described in ref 32. The friction tests were performed on a CSM pin-on-disc tribometer at room temperature. The normal load was set at 2 N. The film-coated Si wafer was fixed on a rotary sample platform using a bare (for test in humid air) or same-film-coated (for test in dry N_2 and H_2) SUJ2 ball of 6 mm in diameter as a counterpart. The rotation radius was 3.5 mm, and the linear sliding speed was 15 cm/s (for test in humid air) or 20 cm/s (for test in dry N_2 and H_2). Different gaseous environments including humid air (22 ± 2% RH), dry inert N_2 and diluent reactive H_2 (40 vol % H_2 + 60 vol % He) were produced by purging water vapor or a distinct gas source into the tribometer chamber until stability was reached before the friction test. The outlet pressure of the gas pipeline was 500 Pa. A Nikon optical microscope and a three-dimensional (3D) white-light interferometer (Zygo NewView 6300) were used to measure the wear morphology and topography. The local microstructure of the polymer-like a-C:H:Si film was characterized by high resolution transmission electron microscopy (HRTEM) operating on a JEOL JEM-2010HC system at 200 kV. Raman spectroscopy (Renishaw System, Ar^+ laser, 532 nm) was employed to detect the carbon bonding state change of a-C:H:Si films before and after the friction test. The bonding chemistry of the as-grown and worn surfaces was detected using imaging 3D time-of-flight secondary ion mass spectrometry (ToF-SIMS, PHI TRIFT III) with a Ga^+ analytical gun as the primary ion source.

3. RESULTS

3.1. Overview of Basic Properties of a-C:H:Si Films upon Bias Voltage. The growth mechanism and structural evolution of a-C:H:Si films with respect to the applied bias voltage (i.e., incident ion energy) has been presented in detail elsewhere.[32] Overall, depending on the ion-surface interactions, the bonding structure of a-C:H:Si films grown in different ion energy regions evolves from hydrogen-rich chain-developed polymer-like (0.25−0.5 kV) to cross-linked diamond-like (1.0−2.5 kV) to hydrogen-deficient sp^2-bonded a-C (3.0−3.5 kV), as revealed by XPS, Raman and FTIR analysis in the previous work.[32] Here, we briefly summarize in Table 1 the basic properties of these films to facilitate understanding of the frictional behaviors studied in this work. With increasing the bias voltage from 0.25 to 3.5 kV, the hydrogen content in the films determined by elastic recoil detection analysis (ERDA) decreases gradually from 36.7 to 17.3 at. %, while the carbon content increases correspondingly from 52.5 to 70.1 at. %. Meanwhile, the Si content is kept almost constant at ∼9−10 at. % for the fixed gas flow ratio of TMS/C_7H_8 during deposition, irrespective of the bias voltage. In addition, a small amount of oxygen (i.e., 1−3 at. %) was present in all the as-grown a-C:H:Si films, as well as some traces of nitrogen remaining in the films. A dynamic smoothening behavior was universally observed for these films grown from energetic ions in a wide range of ion energies, and an atomically smooth surface with

root-mean-square (RMS) roughness of ~0.1 nm was recorded for all these films. The mechanical properties have a close relationship with the film bonding structure. A relatively low hardness (~13−15 GPa) was measured for both polymeric and sp^2-bonded amorphous structures, whereas a higher value (~17−18 GPa) was achieved for the diamond-like film. A similar variation trend depending on the bias voltage is also observed for the measured elastic modulus. Note that, as already declared in ref 32, the hardness of the polymeric samples (~13−15 GPa) is far larger than that of the traditional organic polymers (i.e., ~0.5−2 GPa), but we still call it "polymer-like" due to their high hydrogen content and chain-developed bonding network. All the as-grown films consist of an adherent a-C:H:Si interlayer of 400−500 nm thickness and a bias-voltage-tailored a-C:H:Si top layer. The thickness of the top layer was controlled at around 1.0−1.2 μm. The intrinsic hardness of the top layer was recorded by nanoindentation based on the one-tenth-thickness principle, to avoid any effect from the interlayer or Si substrate. The stress state further confirms the above arguments about ion-energy-controlled bonding structure, that is, the as-grown a-C:H:Si films display significantly low residual stresses (~0.8 GPa) in both polymeric and sp^2-bonded a-C films while possessing a relatively high compressive stress (~1.4 GPa) inherent in the hard diamond-like network. The viscoplastic exponent x, an evaluation index for the rheological properties of materials, indicates an enhanced viscous property (i.e., interfacial flexibility) for hydrogen-rich a-C:H:Si films, and obtains a value of ~0.06 for the polymeric sample with H content of 36.7 at. %.[32]

3.2. Hydrogen Dependence of Frictional Behaviors of a-C:H:Si Films in Various Gaseous Environments.

3.2.1. Friction in Dry N_2. The frictional behaviors of a-C:H:Si films tribotested in dry N_2 are shown in Figure 1, which were previously reported in ref 32. Figure 1a indicates the friction coefficient curves from four representative samples containing different hydrogen contents. It can be observed that for all the tested samples the friction coefficient evolves from an intensive running-in period (i.e., initial friction coefficient μ_{in} around 0.5−0.8) into a low-friction steady state. The running-in period differs significantly in the rubbing cycles with regard to the hydrogen content in the films: ~1500 cycles (17.3 at. % H), ~300 cycles (20.5 at. % H), ~75 cycles (31.9 at. % H) and ~55 cycles (36.7 at. % H), respectively. In addition to the prolonged running-in period, a noticeable number of fluctuations in the steady-state friction coefficients (μ_{ss}) are observed for the hydrogen-deficient a-C:H:Si samples (i.e., 17.3 and 20.5 at. % H-containing films). The inset figure shows the magnified friction coefficient curves in the steady state. An extremely low friction coefficient (μ_{ss} ~ 0.001) is recorded for the sample with hydrogen content of 31.9 at. %, implying nearly vanishing of friction upon sliding. The amplitude of variation in the steady-state friction coefficient is ±0.0005, indicating an ultrasmooth rubbing process in the superlubric state for the self-mated a-C:H:Si films. This extremely stable near-frictionless state continued until the end of the test. In comparison, the friction coefficient of an uncoated SUJ2 ball against an uncoated Si wafer was quite unstable and reached a high value in the range of 0.3−0.6 when tested under the same conditions. A slightly increased but still superlow friction coefficient (μ_{ss} ~ 0.006) is also detected for the sample hydrogenated to 36.7 at. %. It seems that the relatively low hardness (~13.8 GPa) of this sample weakens the antifriction performance to some extent when the presence of plentiful tribodebris produced around the contact area is considered, as shown in Figure 2a4 below. In contrast, the friction coefficients obtained from the hydrogen-deficient samples just approach a quasi-superlubric state: 0.019 for 17.3 at. % H and 0.016 for 20.5 at. % H, respectively. Moreover, the amplitude of fluctuations in the friction curves is strengthened with decreasing the hydrogen content in the films, indicating a worsening stability of lubricating state. Figure 1b summarizes the evolution of average μ_{ss} as a function of hydrogen content in the films. There seems to be a hydrogen content threshold (i.e., ~20 at. %) existed for the a-C:H:Si films to achieve superlow friction in dry N_2.

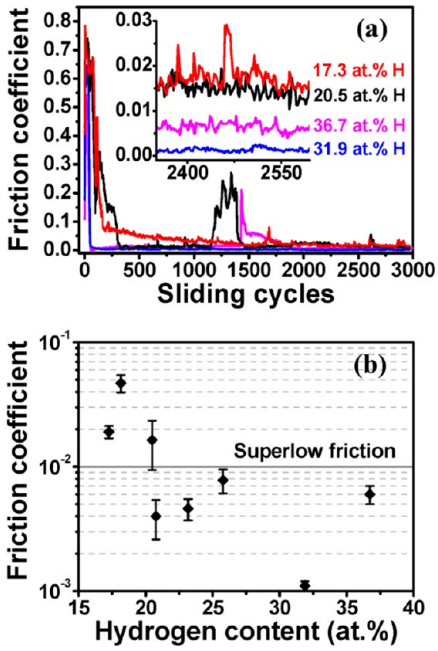

Figure 1. Frictional behaviors of a-C:H:Si films slide against the corresponding film-coated SUJ2 balls in dry N_2: (a) representative friction coefficient curves of samples with different hydrogen contents. Tribotesting conditions: normal load of 2 N, rotation radius of 3.5 mm and sliding speed of 20 cm/s. The inset figure shows the magnified friction curves in the steady state. (b) Hydrogen dependence of the average steady-state friction coefficient, indicating the existence of a superlow friction region when H > 20 at. %. Reproduced with permission from ref 32. Copyright 2014 AIP Publishing LLC.

Figure 2 shows the optical wear morphologies of the sliding pairs in the contact area after the friction tests in dry N_2, as shown in Figure 1. It is obviously seen that white wear scars, barely (a1) or partially (a2−a4) covered by tribolayers, are formed on the film-coated SUJ2 balls. In addition, a large amount of tribodebris is distributed outside the wear scar. Correspondingly, a large number of tribolayers are formed in the wear track (b1−b4) on the film-coated Si substrates. It seems that these tribolayers were mainly transferred from the film materials coated on SUJ2 balls, as will be discussed below. Note that the white color of the wear scars on film-coated SUJ2 balls implies that the wear depth has approached the Fe basement because the ferrite iron usually appears in white color under an optical microscope when the sliding-induced surface polishing effect is considered. This argument is based on the scanning electon microscopy-energy-dispersive X-ray spectroscopy (SEM-EDS) analysis below.

The above results clearly indicate that the frictional performances of a-C:H:Si films in dry N_2 are highly dependent on the hydrogen content in the films, which are similar to what

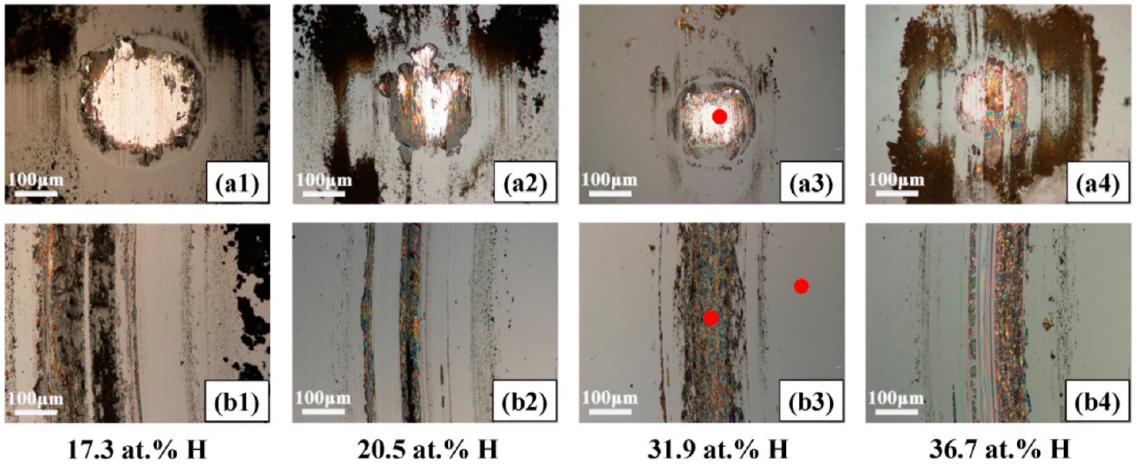

Figure 2. Wear morphologies of the sliding pairs after the friction tests in dry N_2 as shown in Figure 1: (a1−a4) wear scars on the film-coated SUJ2 balls and (b1−b4) the corresponding wear tracks on the film-coated Si substrates with hydrogen contents of 17.3, 20.5, 31.9 and 36.7 at. % in the films, respectively. The red dots marked in panels a3 and b3 indicate the positions for Raman analysis, as will be discussed in the text.

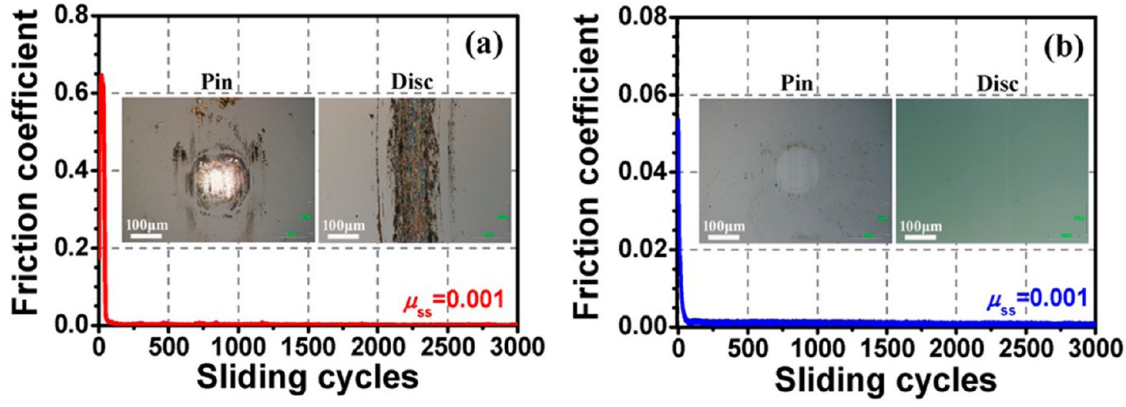

Figure 3. Comparison of near-frictionless behaviors and the corresponding wear morphologies of both the polymeric a-C:H:Si (31.9 at. % H) and a-C:H (~40 at. % H, grown from pure C_7H_8 at 0.25 kV in the same ionization system used in this work) films in dry N_2: (a) self-mated sliding of a-C:H:Si (31.9 at. % H) under 2 N at a speed of 20 cm/s, and (b) self-mated sliding of a-C:H (~40 at. % H) under 10 N at a speed of 15 cm/s. An extremely low friction coefficient of 0.001 was achieved for both cases, while the contact morphologies (inset images) were totally different (see discussions in the text). Note that the friction curve and wear morphologies for the a-C:H:Si (31.9 at. % H) film in panel a are from Figures 1a and 2a3,b3.

have been found in near-frictionless carbon (NFC) films by Erdemir.[9−11] In Erdemir's work, the hydrogen content in a-C:H films could be controlled by varying the source gas composition of H_2 + CH_4 in the plasma during the plasma-enhanced chemical vapor deposition (PECVD) process. The lowest friction coefficient (μ_{ss} ~ 0.001) in dry N_2 was achieved for the highly hydrogenated (39 at. % H) a-C:H films grown from a 75% H_2 + 25% CH_4 gas precursor. Further increase of hydrogen content in the film to 45 at. % (grown from 100% CH_4) weakened the antifriction properties of a-C:H film to some extent, and the friction coefficient increased to ~0.014.[9−11] Similarly, in the present work, the most stable and lowest friction coefficient (μ_{ss} ~ 0.001) in dry N_2 was recorded for the 31.9 at. % H-containing a-C:H:Si film, whereas an increased friction coefficient (μ_{ss} ~ 0.006) was observed for the sample with a maximum hydrogen content of 36.7 at. %. For both a-C:H and a-C:H:Si films, the superlubric state is more likely to appear when the film structure evolves into hydrogen-rich polymer-like. However, the most noticeable difference between these two cases is that almost no visible tribolayer could be found in the sliding areas for NFC self-mated contacts, even though this tribopair also suffered an initial high friction in the running-in period.[10] It seems that the hydrocarbon network in the pure a-C:H film is stiff enough to bear the initial high contact pressure (i.e., a peak Hertz pressure of ~1 GPa under 10 N in Erdemir's work), and thus to avoid huge material loss in this harsh stage. In comparison, a noticeable tribolayer was formed in the wear track during the initial running-in process for a-C:H:Si self-mated contacts. On one hand, superlow friction is maintained when a high hydrogen content (i.e., 31.9 at. % in this work) is held in a-C:H:Si film. On the other hand, the incorporation of Si into a-C:H matrix seems to weaken the load capacity of the hydrocarbon network. Under the initial high contact pressure (a peak Hertz pressure of 0.68 GPa under 2 N), film material is mainly transferred from the ball side to the Si substrate side, producing a newly restructured tribolayer (Figure 2b3). The possible forming process of this friction-reducing tribolayer is discussed in Section 3.3.1.

It should be mentioned that the occurrence of such an extremely low friction coefficient in this polymeric a-C:H:Si film relies on some key factors. One is contact pressure. In a related work, we synthesized a highly hydrogenated a-C:H film from 100% C_7H_8 gas under 0.25 kV by the same ionization

system used in this work. The hydrogen content in this polymer-like a-C:H film is around 40%. It was found that superlow friction is also feasible in self-mated contact for this polymeric a-C:H film in dry N_2 using CSM pin-on-disc rotary tribometer. Higher contact pressure is favorable for achieving lower friction coefficient. An extremely low and stable value of ~0.001 was obtained when the applied load was 10 N. To assist understanding, we compare this result with that of the polymeric a-C:H:Si (31.9 at. %) film in Figure 3. As seen in Figure 3b for the self-mated a-C:H film grown from pure C_7H_8, wear tracks on the disc side were barely visible (i.e., unmeasurable wear rate), and very mild wear scars were produced on the pin surface. This result is quite consistent with Erdemir's NFC findings for a-C:H films[9−11] in view of the extremely low friction coefficient and wear rate under the same gaseous atmosphere (dry N_2) and comparable contact pressure (a peak Hertz pressure of ~1.15 GPa under 10 N in our case). Note that measuring friction coefficient in the range of 10^{-3} or lower is intractable for most tribometers. Any system error would result in inaccurate outcomes. Therefore, lateral force calibration should be carried out before each friction test. For the sake of reliability, we further conducted free-contact rotations before and after each friction test to ensure that no zero shift occurred for the load cell. The friction coefficient should be zero in this mode because no friction force was produced. Due to the minimum sensitivity of lateral force sensor being a few millinewtons in most macroscopic pin-on disc tribometers (5 mN in our CSM tribometer), measuring a friction coefficient down to 0.001 under a relatively low load such as 1 or 2 N means approaching the detection limit of the sensor sensitivity. Therefore, sliding contact under a higher load such as 10 N would improve the stability of frictional force measurement. However, the antifriction behaviors of this polymeric a-C:H:Si film are pressure-dependent. Superlow friction could not be preserved when the normal load was higher than 2 N, due to the pressure-induced crack failure of the film. This is understandable, considering the relatively low hardness and nanoporous microstructure, as observed by HRTEM in Figure 12, of this hydrogen-rich a-C:H:Si sample. Another important factor affecting antifriction behavior of a-C:H:Si films is the sliding speed. Our preliminary experiments indicate that a sliding speed in the range of 15−20 cm/s is more favorable for achieving the extraordinarily stable and lowest friction coefficient, whereas a rather low speed (i.e., below 5 cm/s) weakens or even completely disables the superlubric performances. The underlying mechanism (i.e., dynamic gas adsorption and removal) needs further investigation.

3.2.2. Friction in Diluent Reactive H_2. Figure 4 shows the frictional performances of a-C:H:Si films tribotested in diluent H_2 gas (40 vol % H_2 + 60 vol % He) in consideration of the lubrication effect of hydrogen. Note that, due to the low density of H_2 gas, the outlet of the gas pipe was placed near the contact area to ensure the presence of sufficient hydrogen on the contact surfaces before it floats upward. The friction coefficient curves from four representative samples with different hydrogen contents are indicated in Figure 4a. Being similar to the case in dry N_2, the friction coefficient evolves into a steady state after an intensive running-in process. Prolonged running-in periods and intensified fluctuations in the friction curves are observed for the H-deficient samples (i.e., 17.3 and 20.8 at. % H-containing films). As shown in the inset figure, extremely low and stable friction coefficients (i.e, 0.003 and 0.005) are

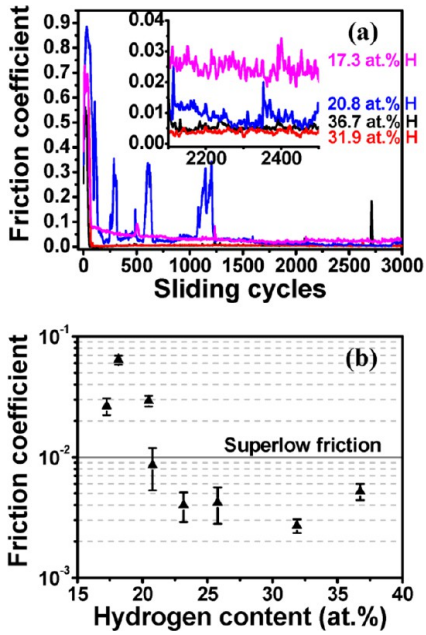

Figure 4. Frictional behaviors of a-C:H:Si films slide against the corresponding film-coated SUJ2 balls in diluent reactive H_2 (40 vol % H_2 + 60 vol % He): (a) representative friction coefficient curves of samples with different hydrogen contents. Tribotesting conditions: normal load of 2 N, rotation radius of 3.5 mm and sliding speed of 20 cm/s. The inset figure shows the magnified friction curves in the steady state. (b) Hydrogen dependence of the average steady-state friction coefficient, indicating the existence of a superlow friction region when H > 20 at. %.

detected for 31.9 and 36.7 at. % H-containing a-C:H:Si films, respectively. As the hydrogen content decreases, the friction coefficient increases close to or exceeding the value of 0.01 (i.e., 0.009 for 20.8 at. % H and 0.027 for 17.3 at. % H). Noticeable fluctuations and instability still exist in the friction curves for these H-deficient samples. The above results imply that superlubricity is not likely to occur even under the lubrication by a hydrogen-providing source such as H_2 if the as-grown film structure is unable to meet some requirements, for instance, sufficient hydrogen inherent in the film or high H-passivating degree on the pristine film surface. Figure 4b summarizes the hydrogen dependence of average μ_{ss} for the as-grown a-C:H:Si films. Superlow friction is feasible in lubricating H_2 for the samples with H content larger than ~20 at. %.

The corresponding wear morphologies of sliding pairs after the friction tests in diluent H_2 are shown in Figure 5. It is observed that a white wear scar without covering by any visible tribolayers is only found on the SUJ2 ball coated by the most H-deficient film (17.3 at. % H, a1), whereas the other three are totally covered by brown tribolayers (a2) or possess smooth contact surface with the color close to the film (a3, a4). This result suggests that the presence of gaseous H_2 can effectively facilitate the formation of tribolayers and protect the contact surfaces upon sliding especially for the films with hydrogen content exceeding a value (i.e., ~20 at. %). As for the film-coated Si substrates, the wear tracks (b1−b4) are covered by continuous tribolayers, which is similar to the case in dry N_2 atmosphere.

3.2.3. Friction in Humid Air. To further evaluate the frictional response to the presence of water molecules, we tested these films in a humid environment with a RH of 22 ±

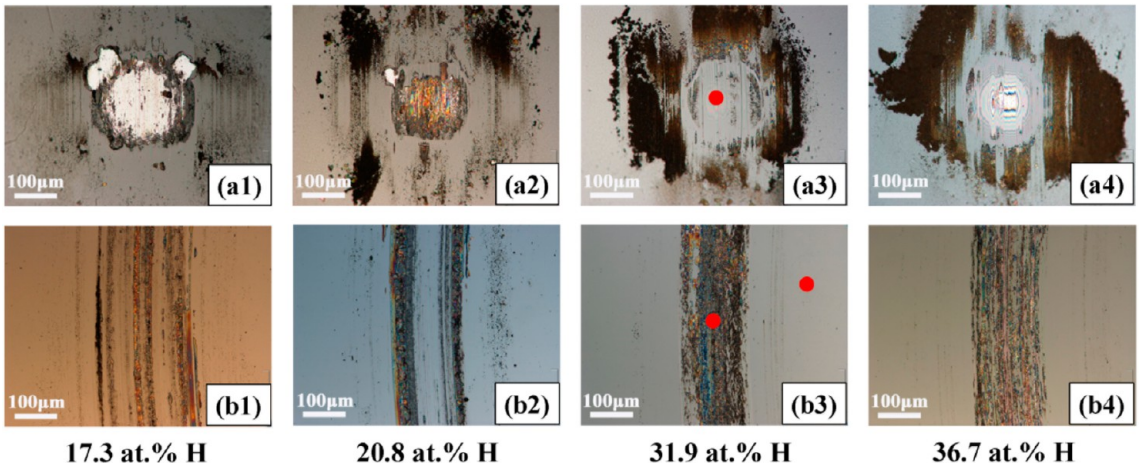

Figure 5. Wear morphologies of the sliding pairs after the friction tests in diluent reactive H_2 as shown in Figure 4: (a1−a4) wear scars on the film-coated SUJ2 balls and (b1−b4) the corresponding wear tracks on the film-coated Si substrates with hydrogen contents of 17.3, 20.8, 31.9 and 36.7 at. % in the films, respectively. The red dots marked in panels a3 and b3 indicate the positions for Raman analysis, as will be discussed in the text.

2%. To be comparable with the previous results,[31] we chose bare SUJ2 balls instead of film-coated ones as counterparts for sliding tests, as shown in Figure 6. The frictional behaviors from

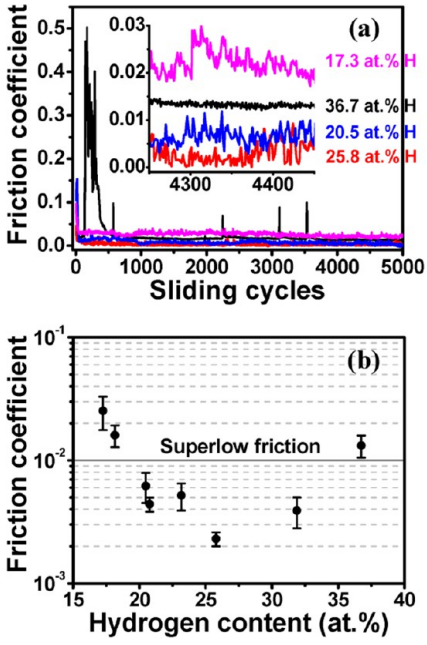

Figure 6. Frictional behaviors of a-C:H:Si films slide against bare SUJ2 balls in humid air (22 ± 2% RH): (a) representative friction coefficient curves of samples with different hydrogen contents. Tribotesting conditions: normal load of 2 N, rotation radius of 3.5 mm, and sliding speed of 15 cm/s. The inset figure shows the magnified friction curves in the steady state, and (b) hydrogen dependence of the average steady-state friction coefficient.

four representative samples with different hydrogen contents are compared in Figure 6a. As noticed, the initial friction coefficients in humid air are significantly reduced for most samples (i.e., $\mu_{in} \sim 0.05-0.15$) except for the film with maximum hydrogen content (i.e., $\mu_{in} \sim 0.5$). In addition, the running-in period is shortened, and no sharp fluctuations, as found for the hydrogen-deficient samples in dry N_2 and H_2, are observed in the whole sliding process. It is obviously seen from the inset figure that superlow friction is feasible for the samples hydrogenated to some extent (i.e, 25.8 and 20.5 at. %), whereas the most polymeric (36.7 at. % H) and H-deficient (17.3 at. % H) samples just achieve a quasi-superlubric state ($\mu_{ss} \sim 0.013$) and an ultralow friction ($\mu_{ss} \sim 0.025$), respectively. It indicates that, in addition to the Si−OH passivating group, H-termination is also involved in achieving superlubricity in humid air. The steady-state friction curve of the polymeric sample (36.7 at. % H) is very smooth, which is an indirect hint for the passivation effect of H on the contact surface. Note that the superlow friction curves obtained in humid air for a-C:H:Si films (i.e, 25.8 and 20.5 at. % H) display a lot of tiny fluctuations, which is indicative of a more complex surface-gas interaction process in this condition. Figure 6b indicates the hydrogen dependence of μ_{ss} for all the as-grown a-C:H:Si films. It is seen that superlow friction is more feasible for the films with an appropriate hydrogen content (i.e., 20−35 at. %).

The wear morphologies of the sliding pairs corresponding to the tests in Figure 6 are shown in Figure 7. Overall, the wear morphologies in humid air are totally different from those obtained in dry N_2 or diluent H_2. As shown in Figure 7a1−a4, white wear scars are not found in the contact areas for the bare SUJ2 balls. Instead, a large number of tribolayers are distributed in the center of wear scars or around the contact areas. It seems that these tribolayers were mainly transferred from the film materials coated on Si substrates to the bare SUJ2 ball surfaces, which is contrary to the case in dry N_2 or H_2. Correspondingly, worn tracks (b1−b4) are produced on the film-coated Si substrates. As reported previously,[31] the dissociative formation of hydrophilic silicon oxide layers (Si−OH) between the contact surfaces along with the adsorbed boundary water layer is the origin of ultralow friction for a-C:H:Si films in humid air. The present results demonstrate that hydrogen might also participate in either shielding the film surfaces from or reacting with the surrounding gaseous medium such as H_2O molecules. The combined function of all these factors finally determines the frictional behaviors of a-C:H:Si films in humid air. However, at present, we do not have direct evidence for the argument of the shielding effect of hydrogen on hydrophilic contact surfaces in humid air. Further work such as molecular dynamics simulations is necessary to uncover this query.

3.3. Origin of Superlubricity in Polymer-like a-C:H:Si Film. *3.3.1. Tribolayer Formation on Contact Surface.* The

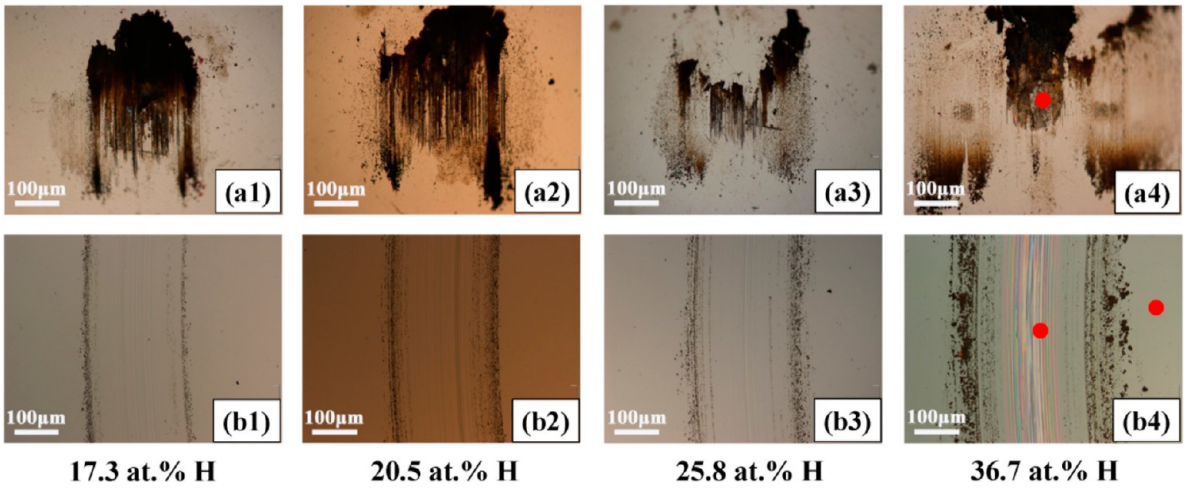

Figure 7. Wear morphologies of the sliding pairs after the friction tests in humid air as shown in Figure 6: (a1−a4) wear scars on bare SUJ2 balls and (b1−b4) the corresponding wear tracks on the film-coated Si substrates with hydrogen contents of 17.3, 20.5, 25.8 and 36.7 at. % in the films, respectively. The red dots marked in panels a4 and b4 indicate the positions for Raman analysis, as will be discussed in the text.

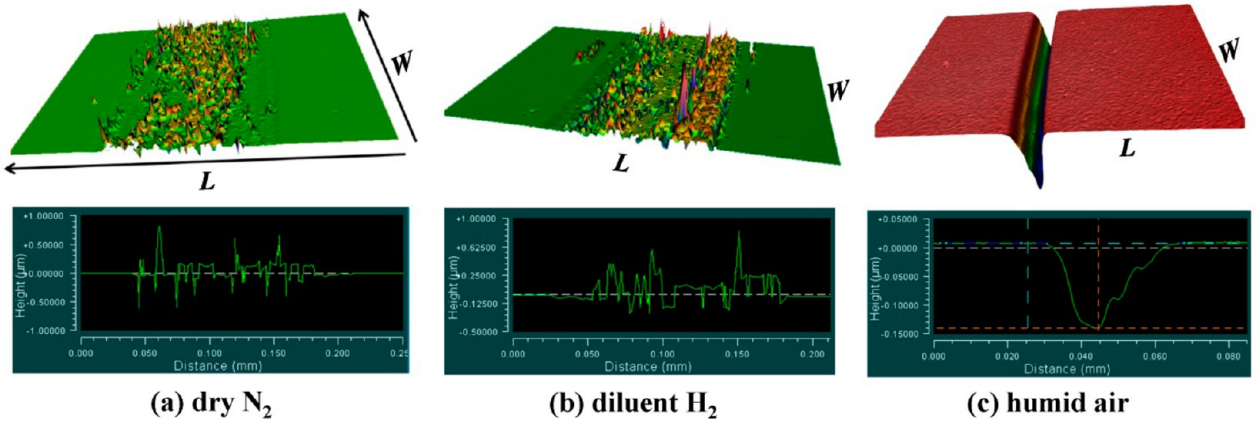

Figure 8. Three-dimensional morphologies (upper portion) and cross sections (lower portion) of wear tracks formed on the polymeric-film-coated Si substrates with hydrogen content of 31.9 at. % in the film after the friction tests in (a) dry N_2, (b) diluent H_2 and (c) humid air, respectively. Scan size: L = 350 μm, W = 260 μm. Scale bars in each cross-sectional image are as follows: (a) 0.5, (b) 0.375 and (c) 0.05 μm per major tick in the vertical height axis, and (a) 0.05, (b) 0.05 and (c) 0.02 mm per major tick in the horizontal distance axis. The white dashed lines in the cross-sectional images indicate the horizontal planes of the original as-grown film. The thickness of the tribolayer or the depth of the wear track can thus be roughly deduced from these morphological profiles.

above results in Section 3.2 depict the superior antifriction performances of the polymer-like a-C:H:Si (31.9 at. %) film compared to other samples in the three gaseous atmospheres, especially in dry N_2. Therefore, the following work mainly focuses on the lubrication mechanism of this polymer-like a-C:H:Si film. To gain further insight into the relationship between tribolayer formation and frictional behaviors of a-C:H:Si films, a white-light interferometer was first utilized to characterize the topographical features of the contact surfaces. Figure 8 shows the three-dimensional morphologies and cross sections of wear tracks from the a-C:H:Si (31.9 at. %) sample after the friction tests in the three gaseous atmospheres. Two distinct types of wear morphologies can be distinguished with respect to the tribotesting condition. In both dry N_2 (Figure 8a) and diluent H_2 (Figure 8b), a tribolayer with an average thickness of ∼100−200 nm is found to uniformly cover the wear track, indicating the film material transfer from film-coated ball surface to film-coated Si substrate. This tribolayer is exactly located in the center of the contact areas rather than squeezed out from the wear track. Very little tribodebris can be found on the edge of the wear track. Therefore, this newly formed tribolayer is directly involved in the rubbing process throughout the experiment to eliminate friction between the two contact surfaces. The present observed formation and distribution of tribolayer during sliding is quite consistent with recent large-scale molecular dynamics simulations of wear in DLC films by Sha et al.[33] A tribolayer covering the wear track is also found to be formed for DLC self-mated contacts in the running-in period through the material loss from the ball side by a cluster detachment process. Due to the high stress localization at contact point on the ball side, lateral mass transport evolves along the interface toward the trailing edge of the sliding asperity. Consequently, material detachment occurs due to strong chemical bonding across the interface, and a newly restructured tribolayer is formed on the opposing flat surface.[33] At present, we cannot completely understand how this tribolayer is working to eliminate friction for the polymeric a-C:H:Si film during the rubbing process, especially when considering the roughness of these tribolayer-covering contact surfaces increased to a noticeable extent (Figure 8a,b) as

compared with the original as-grown ultrasmooth surface. This is totally different from the near-wearless and smooth contact surfaces after the friction test in Erdemir's NFC a-C:H films[9−11] or in our C_7H_8-grown superlubric a-C:H film (Figure 3b). The most likely scenario we speculate is that these tribolayers are acting as lubricating "tribo-polymers", which are soft and flexible byproducts due to tribochemical polymerization during sliding contact. The presence of tribo-polymers for friction reduction was also reported by other researchers.[34−36] This is reasonable when considering the hydrogen-rich polymeric and nanoporous characteristic (TEM results in Figure 12) of the original a-C:H:Si film, the enhanced photoluminescence background (Raman results in Figure 16a,b) and the hydrocarbon-rich fragmentation (ToF-SIMS results in Figure 17) of these tribolayers after the friction test. During sliding, these tribolayers are flexible and conformal at each contact asperity (i.e., local smoothening effect) to accommodate the lateral movements of the interface and to lower the friction, rather than to increase friction by acting as hard third bodies. In comparison, a typical abrasive groove (Figure 8c) is found on the wear track after the friction test in humid air, implying that the film material was mainly transferred to the bare SUJ2 ball surface for tribolayer build-up as observed in Figure 7.

As shown in Figure 1a, the establishment of an extremely low friction state ($\mu_{ss} \sim 0.001$) after the running-in period in dry N_2 signifies a subsequent stable rubbing process and minimal material transformation between contact surfaces. Thus, it is highly necessary to determine the role of the running-in process in tribolayer formation. For this purpose, we substantially shortened the total sliding cycles to 200 and retested this polymer-like a-C:H:Si film in dry N_2. Figure 9 shows the friction curve of 200-cycle case along with the first 300 cycles of the case run for total 3000 cycles as already shown in Figure 1a, and the corresponding wear morphologies of the sliding pair. It is seen that good reproducibility of suplerlow friction (Figure 9a) can be obtained in dry N_2, and both the friction coefficients evolve quickly into a superlow region ($\mu_{ss} \sim 0.001-0.002$) after a high-friction running-in period with sliding cycles of ~75. The wear morphologies of the contact pair after 200-cycle sliding (Figure 9b,c) are similar to the case of 3000 cycles, as shown in Figure 2a3,b3. The measured diameter of the wear scar on a film-coated SUJ2 ball and width of the tribolayer track on a film-coated Si substrate in the case of 200-cycle sliding are quite close to that of 3000 cycles: 216.9 μm (200 cycles) vs 226.3 μm (3000 cycles) and 197.8 μm (200 cycles) vs 206.5 μm (3000 cycles), respectively. These results demonstrate that the friction-reduction tribolayer on contact surfaces is mainly formed during the running-in period rather than in the steady state.

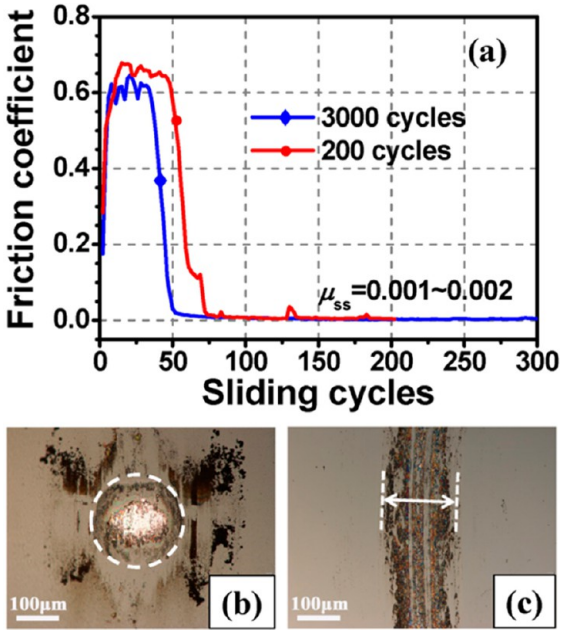

Figure 9. (a) Friction curve of the a-C:H:Si (31.9 at. % H) self-mates run for total 200 cycles in dry N_2, along with the first 300 cycles replotted from the case run for total 3000 cycles as shown in Figures 1a and 2a3,b3, and the corresponding (b) wear scar on film-coated SUJ2 ball and (c) wear track on film-coated Si substrate. Tribotesting conditions: normal load of 2 N, rotation radius of 3.5 mm and sliding speed of 20 cm/s.

Counterface material is acting as another important factor controlling tribolayer formation and tribochemical state between sliding interfaces. Figure 10 compares the frictional behavior of the polymeric a-C:H:Si (31.9 at. % H) film run in self-mate with that slide against bare SUJ2 ball in dry N_2. It is obviously seen from Figure 10a that running against bare SUJ2 significantly prolongs the running-in period to ~750 cycles as compared to ~75 cycles in self-mate. Furthermore, the μ_{ss} finally stabilizes at a quasi-superlubric value of ~0.013 instead of a superlow one, such as ~0.001 in the case of self-mate. A large amount of black-brown tribodebris is accumulated around the wear scar on the bare SUJ2 ball surface, as shown in Figure 10b, indicating the continuous lubrication effect through material transfer from a-C:H:Si film on Si substrate. In comparison, a uniform black-brown tribolayer, as observed in the case of self-mate (Figures 2b3 and 8a), is no longer found

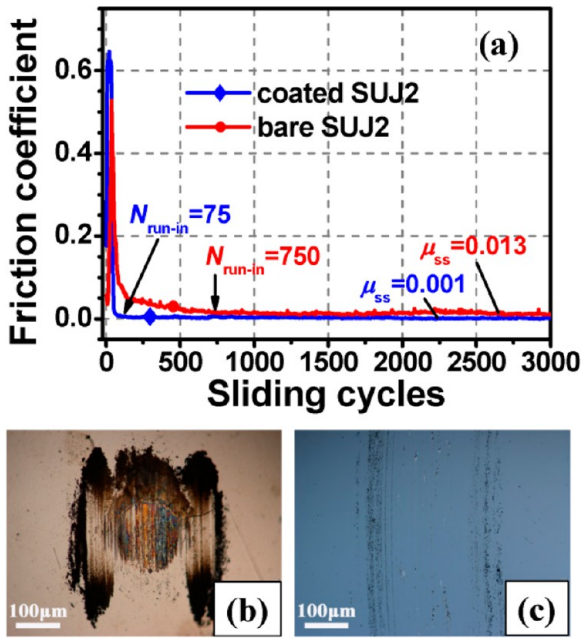

Figure 10. (a) Frictional behavior of the polymer-like a-C:H:Si (31.9 at. % H) film coated on Si substrate run against bare SUJ2 ball in dry N_2, along with the self-mated case as already shown in Figures 1a and 2a3,b3, and the corresponding (b) wear scar on bare SUJ2 ball and (c) wear track on film-coated Si substrate. Tribotesting conditions: normal load of 2 N, rotation radius of 3.5 mm, and sliding speed of 20 cm/s.

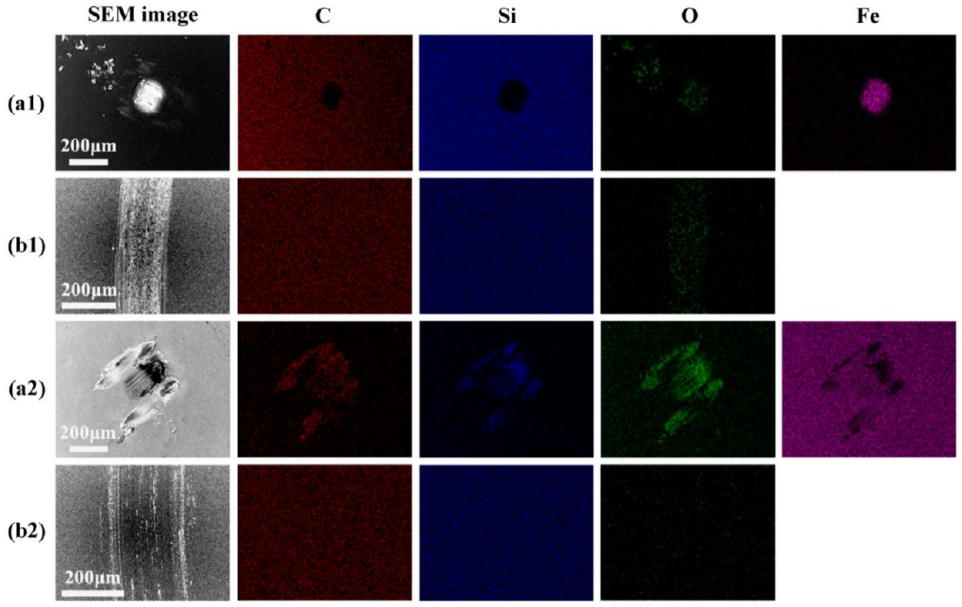

Figure 11. SEM-EDS mapping of the contact surfaces after sliding in self-mates and against bare SUJ2 ball for the polymer-like a-C:H:Si film (31.9 at. % H) in dry N_2: (a1) wear scar as shown in Figure 2a3, (b1) wear track as shown in Figure 2b3, (a2) wear scar as shown in Figure 10b and (b2) wear track as shown in Figure 10c.

on the wear track surface in the present case (Figure 10c). The counterpart, SUJ2 bearing steel, is a high-carbon chromium alloy steel and the main chemical composition is as follows: C (0.95−1.05%), Cr (1.3−1.6%), Si (0.15−0.35%), Mn (0.25−0.45%) and other trace elements (P, S, Mo, Ti, Cu). To further elucidate the chemical state on contact surfaces, we performed SEM-EDS mapping analysis on the polymeric a-C:H:Si film (31.9 at. %) after sliding in self-mate or against bare SUJ2 ball in dry N_2. Four elements including C, Si, Fe and O were chosen as detecting objects, and the results are shown in Figure 11. For self-mate, the wear scar surface is lacking in C and Si and rich in Fe (Figure 11a1), implying deep removal of film material coated on the SUJ2 ball surface during sliding. This is consistent with the optical observation results as shown in Figure 2. However, it should be pointed out that the weak signals of C and Si are not representative of complete absence of a friction-reducing tribolayer on the wear scar surface, especially when in view of the superlow friction ($\mu_{ss} \sim 0.001$) obtained in this condition. The thickness of this tribolayer is expected to be quite small such as at the nanoscale, since recent experiment has found that the HRTEM confirmation of a very thin (~10 nm) carbon tribolayer formed on the wear scar of ball surface is enough for achieving stable and low friction for CN_x coatings in a dry inert gas.[37] In addition, the considerable signal reinforcement of O is expected to come from the water adsorption on the porous polymer-like tribolayer (as will be discussed below) when exposing to the air during sample transfer after the friction test in dry N_2. The tribolayer formed on the wear track surface almost maintains the elemental composition of the as-grown film in view of the uniform signal distribution of C and Si, as shown in Figure 11b1. The distinguishable signal reinforcement of O is derived from the same reason as mentioned above. For the case of sliding against the bare SUJ2 ball, the significantly intensified signals of C, Si and O in the contact area in Figure 11a2 demonstrate the covering of wear scar on iron surface by carbon-rich tribolayers. The uniform weak signal of O on the wear track surface (Figure 11b2) confirms the very thin thickness of the black-brown tribolayer, as observed in Figure 10c. The above results indicate that self-mated sliding is more effective in achieving superlow friction due to quick tribolayer build-up (i.e., running-period just lasting for ~75 cycles). In comparison, the pristine SUJ2 ball surface is generally covered by adventitious carbon and iron oxide layers. The existence of such oxide layers seems to slow the tribolayer growth and thus affect the final rubbing state, as also observed by other researchers.[38]

3.3.2. Local Microstructure and the Role of Hydrogen in Lubrication. The above results demonstrate that the superior antifriction performances of hydrogen-induced polymer-like a-C:H:Si (31.9 at. % H) film should have a close relationship with their bonding structure and the subsequently formed tribolayers on contact surface during sliding. However, the local microstructure of this polymeric a-C:H:Si film, especially the bonding state of hydrogen in the film, and its specific role in the lubrication progress, remain unclear. Thus, we provide direct observation of the local microstructure of this polymeric a-C:H:Si film by HRTEM, as shown in Figure 12a. It is seen that the as-grown a-C:H:Si film was tailored to possess a bilayer structure, in which a 1.1-μm thick polymer-like a-C:H:Si layer was deposited on top of a 0.5-μm thick diamond-like a-C:H:Si interlayer. This interlayer is effective in improving the bonding strength of the film to the bottom Si substrate as well as in acting as a load support layer, due to their relatively high hardness (~23 GPa), for the top polymeric layer. The HRTEM image in Figure 12b shows the continuous and dense boundary interface formed between the diamond-like and the polymer-like individual layers. Note that an obscure phase contrast can also be observed between them, indicating a disparity in composition and bonding structure. The local nanostructure of the top polymer-like layer is further indicated in Figure 12c. It seems that a large number of nanoscale pores with diameter of ~0.5−1.0 nm are evenly distributed in the film. Such a nanoporous structure is thought to be developed under low energy subsurface growth from a hydrogen-rich ion flux produced in the ionization system.[32] Several early studies have also reported the presence of microvoids in silicon-related

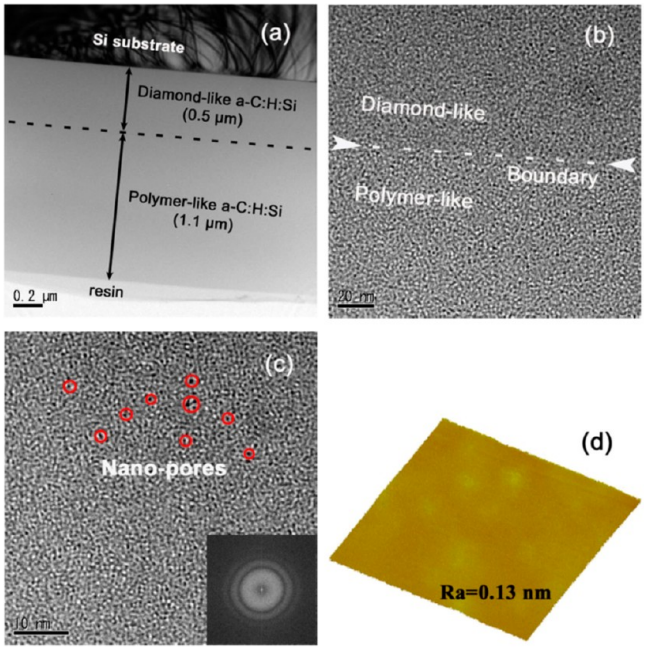

Figure 12. Nanostructure of the as-grown a-C:H:Si (31.9 at. % H) film. (a) Cross-sectional HRTEM image showing the bilayer structure: diamond-like a-C:H:Si interlayer and polymer-like a-C:H:Si top layer. (b) HRTEM image indicating the continuous and dense boundary between the diamond-like and polymer-like individual layers. (c) HRTEM image showing the local nanostructure of the polymer-like a-C:H:Si top layer. A large number of nanoscale pores (indicated by red circles) are observed to be evenly distributed in the film. The lower inset shows the corresponding FFT image of the film. (d) 2.5 × 2.5 μm^2 AFM morphology image showing the ultrasmooth surface with atomic scale roughness *Ra* = 0.13 nm.

materials such as hydrogenated amorphous silicon (a-Si:H) film and hydrogenated amorphous silicon−carbon (a-$Si_{1-x}C_x$:H) alloys.[39−41] It is estimated by nuclear magnetic resonance (NMR)[40] or small-angle X-ray scattering (SAXS)[41] that these microvoids have a volume size of ∼1 nm in diameter. These nanopores are expected to act as reservoirs for trapped molecular H_2, which are formed from recombination of abundant hydrogen atom during low-energy ion penetrating.[32] The previous work has confirmed several characteristic infrared vibration bands in the film by Fourier transform infrared spectroscopy (FTIR), including Si−C stretching modes, Si−H_n bending and stretching modes and C−H_n stretching modes, as well as some hydrogen-terminating groups such as Si-CH_2 and Si-CH_3.[32] Such a hydrogen-induced infrared vibration is definitely an indicator for the chain-developed polymeric structure in the a-C:H:Si film. It is previously suggested in a-$Si_{1-x}C_x$:H films that hydrogen is mainly incorporated into the films at positions interrupting bonds of the host matrix. Above a certain content of hydrogen, the amorphous network will partly lose its connectiveness so that microvoids are formed. The H-containing species such as molecular H_2, Si−H_n and C−H_n radicals are then trapped in the microvoids or bonded to the microvoid internal surfaces.[39] However, the present HRTEM result still cannot serve as the direct evidence for the existence of molecular H_2 in the film. Other assistant techniques such as NMR and SAXS are necessary to disclose this issue. However, the experimental confirmation of molecular H_2 in the film is quite a difficult task to conduct. Related work is now in progress. The diffuse rings from the Fast Fourier Transform (FFT) diffraction patterns inset in Figure 12c clearly indicate the amorphous characteristic of the polymeric a-C:H:Si film. Moreover, it is important to notice an atomically smooth and featureless surface for the as-grown film, as shown in Figure 12d, with a root-mean-square (RMS) roughness of 0.13 nm. The origin of ultrasmoothness of a-C:H:Si films grown in the present deposition system has been published elsewhere.[32] Such a surface ultrasmoothness, to the greatest degree, would reduce the mechanical interactions between the contact surfaces during sliding for the lubricating materials.

The visible Raman spectra in Figure 13a further indicate that both the diamond-like a-C:H:Si interlayer and the polymer-like a-C:H:Si top layer have an amorphous carbon bonding characteristic. The shrinking of D peak (deriving from vibration modes of sp^2 atoms in aromatic rings) implies the suppression of ring-like structure by Si incorporation.[32] However, the enhanced photoluminescence (PL) background of the polymer-like top layer compared to the diamond-like interlayer obviously reflects the high hydrogen content and chain-developed structure in this layer.[42] The above HRTEM result gives an insight into the possible residing form of hydrogen in the bulk of the polymer-like a-C:H:Si film. In spite of this, we still need to know the accurate bonding state of hydrogen on the film surface because the interfacial property of a film significantly governs the friction and wear behaviors when directly brought into contact sliding. Therefore, the surface chemistry was further detected using an imaging 3D ToF-SIMS, which can provide extra information about the chemical nature of very thin (a few Å to 1−2 nm) surface layers. As shown in Figure 13b, in addition to abundant hydrogen fragments (H), a large number of hydrocarbon fragments (i.e., C_1H_n, C_2H_3, C_3H_n, C_4H_n, C_6H) and Si-containing fragments (i.e., Si, SiH) are also found to exist on the top surface of a-C:H:Si film. This

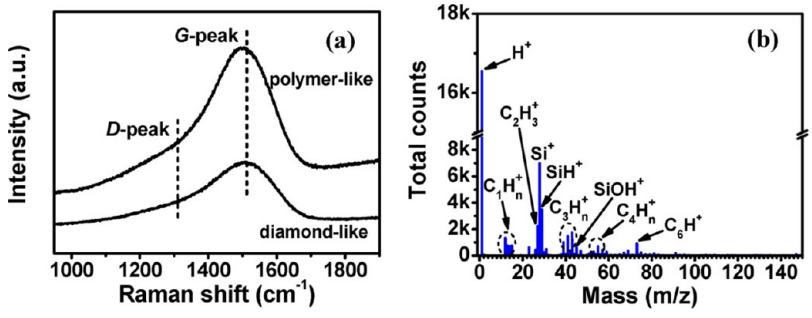

Figure 13. (a) Raman spectra of the diamond-like a-C:H:Si interlayer and the polymer-like a-C:H:Si top layer as shown in Figure 12, and (b) ToF-SIMS fragment ion spectrum showing the chemical composition detecting from the as-deposited surface of the polymer-like a-C:H:Si top layer.

strongly suggests that the original surface of a-C:H:Si film is predominantly passivated by hydrogen atoms, yielding a chemical inertness interface if serving as a sliding counterpart.

As well documented, the low friction between two hydrogen-passivated carbon surfaces in dry inert gas is attributed to the electrostatic repulsive forces[8−11,28] or, recently proposed, the antibonding orbital interactions produced between different atoms at the sliding interface.[43] In either mechanism, the saturation of carbon dangling bonds by hydrogen atoms is the key point to maintain low friction for carbon surfaces. On the other hand, the presence of reactive gaseous molecules such as H_2O and O_2 in the surroundings is able to change this passivating state or even release hydrogen atoms from the carbon surface.[44,45] For instance, density functional theory (DFT) calculations have demonstrated that oxygen atoms can chemically modify the surface stiff C−H bonds by entering between C and H atoms to form C−O−H radicals and thus may increase the friction.[44] Bearing this in mind, we tribotested the polymer-like a-C:H:Si (31.9 at. % H) film in a mixed N_2 + O_2 gas atmosphere by introducing a small amount of O_2 into dry N_2. In addition, a friction test in pure N_2 was also accomplished for comparison. Note that the partial pressure of O_2 flowing around the contact area should be controlled at a level low enough to avoid completely covering the lubrication effect of hydrogen. A pure oxygen or oxygen-rich gaseous atmosphere can dramatically change the frictional behaviors of a-C:H:Si film observed in dry N_2, as will be shown in Figure 15. In the present case, the outlet pressure of N_2 from the gas pipeline was 500 Pa, whereas that of O_2 was set at 20 Pa. The obtained results are shown in Figure 14. As already observed

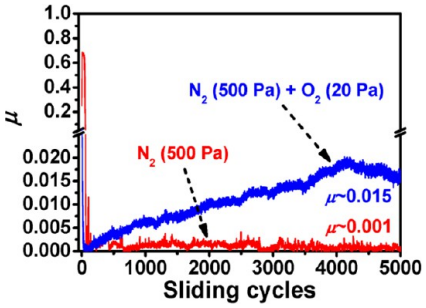

Figure 14. Comparison of frictional behaviors of the polymer-like a-C:H:Si (31.9 at. % H) film tribotested in dry N_2 and mixed gas (dry N_2 diluted by a small amount of O_2), respectively, depicting the pivotal role of hydrogen involved in superlubricity. Tribotesting conditions: normal load of 2 N, rotation radius of 3.5 mm and sliding speed of 20 cm/s.

above, the friction coefficient of the polymer-like a-C:H:Si in pure dry N_2 film quickly evolves into an extremely stable and low value of $\mu_{ss} \sim 0.001$ after a short intensive running-in period. It is reasonable to assume that the rate of hydrogen loss by thermal heating and/or mechanical action during sliding in dry N_2 is very small. In comparison, the presence of a small amount of O_2 in dry N_2 significantly affects the frictional behavior of a-C:H:Si film. The friction coefficient first falls into a superlow scope of ~0.001, resembling the result in dry N_2. However, it gradually increases with the sliding process going on. At around 2000 cycles, the friction coefficient passes over the threshold value of 0.01 and enters into the ultralow scope. Finally, it stabilizes at around 0.015 for the remaining 4000−5000 sliding cycles. The deterioration of superlubric state and gradual increase in friction are therefore correlated with the change of passivation state on contact surface. The most likely scenario is that free hydrogen exists within the film (i.e., nanopores), serving as a reservoir, and it can replenish or replace those surface hydrogen atoms that may have been released by oxygen. The continuous consumption or even exhaustion of free hydrogen inevitably results in a gradual increase in friction, as the available hydrogen cannot effectively terminate those newly produced dangling bonds. However, the present results still cannot serve as the direct evidence for the molecular hydrogen existed in the polymeric structure of a-C:H:Si film. Further work is now in progress to uncover this critical issue.

3.3.3. Evolution of Chemical Bonding upon Sliding Contact in Multienvironments. To further evaluate the frictional behaviors in more wide environments, dry Ar and O_2 have been added as the background atmospheres. The friction tests were carried out using the same parameters as described above. Note that the outlet pressure of O_2 is now 500 Pa. For the convenience of comparison, the friction curves are plotted along with the friction results in dry N_2, diluent H_2 and humid air as shown in Section 3.2. The results are indicated in Figure 15. The average steady-state friction coefficients in each

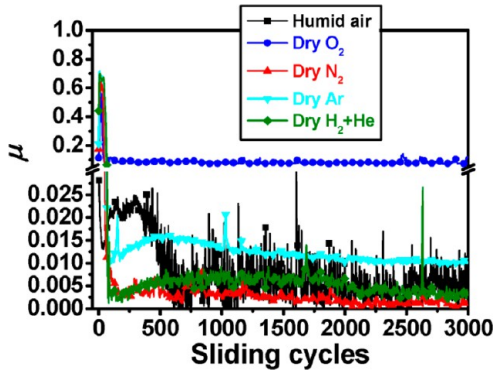

Figure 15. Evolution of friction coefficient vs the number of sliding cycles, of the polymer-like a-C:H:Si film (31.9 at. % H) tribotested in multienvironments including humid air (22 ± 2% RH), inert N_2 and Ar gases, reactive gas H_2 (40 vol % H_2 + 60 vol % He) and corrosive gas O_2. The outlet pressure of each individual gas source was 500 Pa. Tribotesting conditions: normal load of 2 N, rotation radius of 3.5 mm and sliding speed of 20 cm/s (for dry N_2, Ar, O_2 and diluent H_2) or 15 cm/s (for humid air). Note that the friction results in dry N_2, diluent H_2 and humid air are replotted from Section 3.2.

condition are 0.004 (RH22%-air), 0.001 (dry N_2), 0.012 (dry Ar), 0.003 (40 vol % H_2 + 60 vol % He) and 0.084 (dry O_2), respectively. The most stable and lowest value ($\mu_{ss} \sim 0.001$) is achieved in dry N_2. In comparison, the friction coefficient obtained in another inert gas (dry Ar) just approaches a quasi-superlubric state ($\mu_{ss} \sim 0.012$). This difference clearly demonstrates that the molecular diversity even for similar kinds of gas can have a profound effect on the frictional behaviors of a-C:H:Si film. Furthermore, the a-C:H:Si film exhibits noticeably increased but still ultralow friction ($\mu \sim 0.084$), even in the corrosive gas O_2. Overall, this polymer-like a-C:H:Si film possesses superior antifriction properties and can exhibit superlow or ultralow friction in quite wide service environments.

To gain deep insight into the bonding state of the contact area, Raman spectroscopy was utilized to detect wear scar on

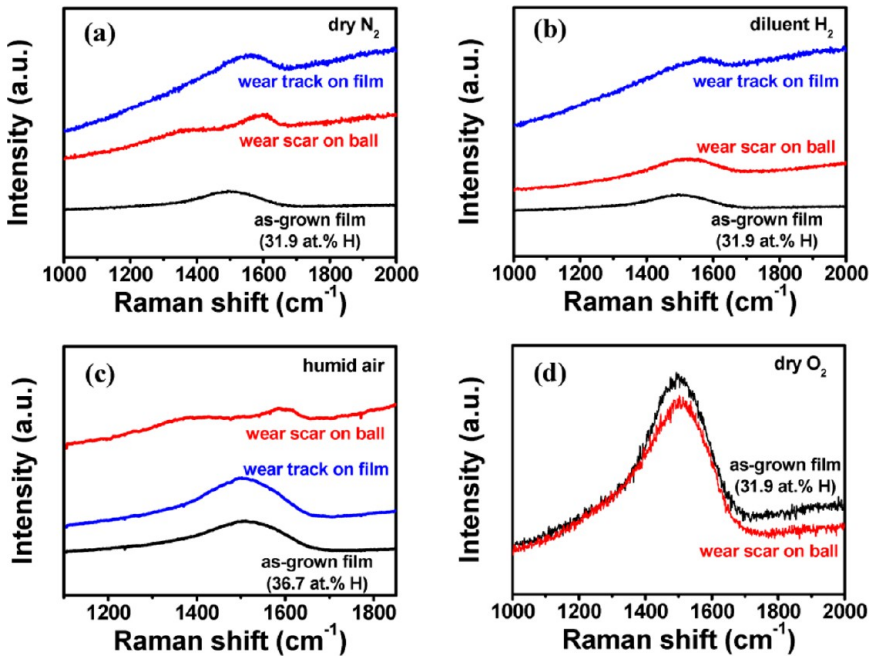

Figure 16. Comparison of carbon bonding states characterized by Raman spectra from as-grown film, wear scar on ball and wear track on film-coated Si substrate for the polymer-like a-C:H:Si film after the friction tests in four representative gaseous environments: (a) dry N_2, (b) diluent H_2, (c) humid air and (d) corrosive O_2. The detecting positions are indicated in Section 3.2.

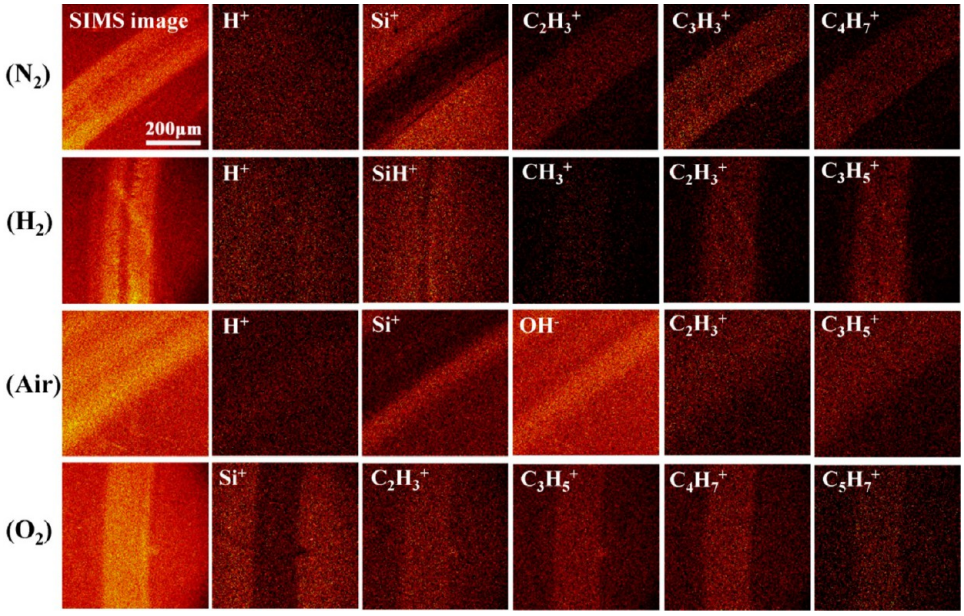

Figure 17. 2D ToF-SIMS images of main fragment ions indicating the surface chemical bonding state of wear track for the polymer-like a-C:H:Si film (31.9 at. % H) after the friction tests (as shown in Figure 15) in multienvironments including dry N_2, diluent H_2, humid air and corrosive O_2.

ball, wear track on film and the as-grown film for the polymer-like a-C:H:Si film after friction tests in four representative gaseous environments, as shown in Figure 16. In dry N_2 (Figure 16a), the Raman spectrum taken from the wear scar on ball (Figure 2a3) splits into two obvious D and G peaks as compared to the as-grown film. The enhancement of the D peak indicates the increase in ring-like structure of sp^2 carbon bonding.[42] Because the film material was, to a large extent, lost from the Fe surface during sliding (Figures 2a3 and 11a1), the Raman signal is mainly from the thin tribolayer formed on the wear scar surface and exactly reflects the nature of it. The Raman spectrum taken from the wear track on film (Figure 2b3) is similar to that of wear scar. However, the D peak is enveloped in the broad band with the G peak. This is because the Raman signal also comes from the underlying as-grown film layer in addition to the top tribolayer formed in the wear track. Another noticeable point is the significantly enhanced PL background in both Raman curves. The exact origin is not yet well understood. It could be, most probably, due to the loose and porous structure of the formed tribolayars, which would increase the defect density and therefore activate the photoluminescence.[46] In diluent H_2 (Figure 16b), the major difference in Raman curve shape is the almost absence of the D peak, even for the signal from the wear scar on ball surface

(Figure 5a3). This finding emphasizes the suppressed formation of a ring-like bonding structure in the thin shear interface when molecular hydrogen is surrounding the contact surface. Hydrogen is likely to chemically react with the top sliding surface under contact pressure and saturate the sp^2-C bonds existing on the interface. In humid air (Figure 16c), the tribolayer formed on the bare SUJ2 ball surface (Figure 7a4) is also rich in sp^2-C, especially the increase in aromatic structure. However, Raman spectrum cannot provide detailed information about the hydrophilic passivation state induced by dissociative adsorption of water molecules on the Si−OH group, which has already been confirmed in the previous work.[31] Thus, the friction reduction in humid air for polymeric a-C:H:Si film is actually from the joint effects of sp^2 phase shear, hydrogen termination and water passivation. In comparison, Raman spectrum taken from the wear scar on film-coated ball surface after the friction test in dry O_2 (Figure 16d) exhibits reduced PL background, implying an H-deficient bonding structure at the sliding interface.

Because a Raman spectrum mainly provides carbon bonding information from the bulk, ToF-SIMS was further used to detect the chemical state, for a wide range of species including hydrogen, of the topmost surface of tribolayers formed in the wear track on Si substrate. The results are shown in Figure 17. In dry N_2, the wear track surface (Figure 2b3) is uniform in H but lack in Si. This means that the contact surface maintains a high content of hydrogen, along with an aromatic-rich structure (as confirmed in Figure 16a) in this very thin shear layer. Thus, the bonding structure in this very thin region of the tribolayer is more like a highly hydrogenated graphite-like carbon, referred as GLCHH, as previously proposed by some researchers.[42] The origin of Si-deficiency in this localized layer is still unclear now. In addition, the strengthened signal of some hydrocarbon fractions such as C_2H_3, C_3H_3 and C_4H_7 in the wear track confirms the existence of a hydrogen-rich top surface layer. In diluent H_2, the wear track (Figure 5b3) is totally covered by hydrogen-terminating groups such as Si−H, CH_3, C_2H_3 and C_3H_5. The increased ratio of H/C in these hydrocarbon groups compared to the case in dry N_2 manifests the passivation effect of molecular H_2 on the contact surface. In humid air, the strong signals of Si and OH radicals confirm the presence of a hydrophilic top layer such as Si−OH at the sliding interface. The formation of such a hydrophilic layer along with adsorption of water molecules provides effective boundary lubrication for friction reduction, as already reported in the previous work for a diamond-like a-C:H:Si film.[31] In the present case of polymer-like a-C:H:Si film, in addition to Si−OH lubrication, hydrogen and some hydrocarbon groups such as C_2H_3 and C_3H_5 are also involved in the rubbing process, indicating a more complex tribochemical process. As for the case in corrosive O_2, oxygen molecules react with Si (more preferentially) and C atoms and simultaneously release part of the surface hydrogen atoms, which results in a more covalent and adhesive top layer containing hydrogen-deficient radials such as C_2H_3, C_3H_5, C_4H_7 and C_5H_7.

4. DISCUSSION

Superlubricity is a quite complex subject in tribology, because its interpretation requires knowledge of various disciplines including materials science, physics, chemistry, solid mechanics, thermodynamics, heat transfer, rheology and so on. The present study has provided some understanding of basic features of superlubricity in a-C:H:Si films. Film bonding structure and environmental medium are the two most influential factors controlling frictional behaviors in amorphous carbon material. Structurally, inclusion of an appropriate amount of silicon into a carbon matrix is effective in suppressing moisture sensitivity of friction in a humid atmosphere, whereas a relatively high content of hydrogen in the films favors friction reduction in dry inert gas. In addition, ultrasmoothness of a film surface guarantees a minimum mechanical interaction between contact surfaces. Environmentally, the molecular characteristic of surrounding gases determines the tribochemistry at the sliding interface, finally altering the frictional response of films during sliding. From a microscopic point of view, this rubbing process involves some key issues such as the phase transformation (i.e., sp^3-to-sp^2 evolution), running-in period, tribolayer formation, pressure-induced bond breaking and formation, hydrogen coverage on the surface, passivation with gaseous species or even shear localization in the very thin top interface.

4.1. Effect of Film Structure. As reported previously, the film structure of a-C:H:Si films grown under different bias voltage evolves from chain-developed polymer-like to cross-linked diamond-like to sp^2-bonded a-C as the hydrogen content gradually decreases from 36.7 to 17.3 at. %.[32] For the mainly sp^3-hybridized polymeric film, the capability to deform and the mobility of such a hydrocarbon chain with their structural arrangements under contact pressure provide a flexible shear deformation at sliding interface.[47] Sufficient hydrogen (i.e., 31.9 at. %) inherent in the as-grown film produces a chemically inert rubbing surface when brought into contact. The most stable and lowest friction coefficient ($\mu_{ss} \sim 0.001$) in dry N_2 is realized in this film. However, excessive hydrogen incorporated in the film (i.e., 36.7 at. %) causes a softening of the film structure. This renders the film fragile by undergoing larger strain and severe bond breaking under an applied load in view of the plentiful tribodebris around the contact area (Figures 2a4 and 5a4), which worsens the superlubric state. For the diamond-like films, superlow friction is still achievable for some of them in dry N_2 (i.e., 20.8−25.8 at. % hydrogenated samples, Figure 1b). Nonetheless, the relatively low hydrogen coverage on the pristine film surface leads to obvious instabilities and fluctuations in the superlubric state even when these covalently cross-linked films are tribotested in diluent H_2 (i.e., 20.8 at. % hydrogenated sample, Figure 4). However, these films exhibit improved wear resistance under lubrication of Si−OH by water molecules in humid air (i.e., 25.8 at. % hydrogenated sample, Figures 6 and 7) due to their higher hardness and elastic constants. Special attention should be given to the mainly sp^2-bonded a-C films, even though these samples cannot achieve superlow friction in all the gaseous atmospheres. But high friction and catastrophic film failure in dry N_2, generally observed for other sp^2-rich materials such as graphite, are not recorded for these films. In contrast, quite stable and ultralow friction is maintained for these hydrogen-deficient films (i.e., $\mu_{ss} \sim 0.02$ for 17.3 at. % hydrogenated sample as shown in Figure 1).

4.2. Running-in for Tribolayer Buildup. Running-in is a key factor controlling the frictional behaviors in a-C films, especially the buildup of friction-reduction tribolayers at the sliding interface.[48−50] MD simulations have revealed that a series of tribochemical reactions occur during this rubbing process, resulting in a remarked restructuring of the film. This restructuring of film involves numerous bond-breaking and bond-forming events occurred within the film (intrafilm) or

between the paired films (interfilm).[51] These events mainly include phase transformation of sp^3-to-sp^2, orientation of bonding structure (i.e., sp^2 rings rotated parallel to the sliding plane), growth of tribolayer, exposing and resaturation of dangling bonds and so on.[52] When the number of bonds broken and reformed reaches a steady-state value, the friction will be lower than that of the initial contact.[53] As shown in Figures 1a and 4a, a high initial friction ($\mu_{in} \sim 0.5-0.7$) is always observed for the polymer-like a-C:H:Si films before entering the superlow friction state in dry N_2 and diluent H_2. However, this running-in period is quite short (lasting for about 75 cycles) but sufficient for the complete buildup of tribolayers at the sliding interface (Figure 9). Moreover, self-mated sliding is more effective in quick development of the friction-reduction tribolayer than sliding against bare SUJ2 ball, as shown in Figure 10. Adventitious carbon and iron oxide layers existed on the counterface ball surface slow the growth of tribolayer. Fontaine et al. reported a strong sticking phenomenon occurring before or at the very beginning of sliding.[38] It was emphasized that the stronger this phenomenon is, the faster is the friction decrease, implying a faster buildup of tribolayers. This is also true in the present case when in view of the higher peak friction of the self-mating case ($\mu_{in} \sim 0.65$) compared to that ($\mu_{in} \sim 0.52$) of sliding against the bare SUJ2 ball (Figure 10).

4.3. Tribochemistry Induced by Environmental Gaseous Molecules. Numerous experimental and simulation studies have emphasized the paramount influence of environmental atmosphere on the frictional behaviors of amorphous carbons.[15,20,21,44,45,54,55] Depending on the chemical characteristics of the gaseous molecules, tribointeractions at the sliding interface can be divided into nonreactive and reactive, respectively. In the case of dry inert gases (such as N_2 and Ar), there are generally no chemical reactions such as dissociative passivation from the surrounding species occurring on the contact surfaces. Therefore, the coupling carbon films should self-lubricate themselves by their as-grown inherent structures to lower the friction. On the other hand, in reactive atmospheres such as O_2, humid air or H_2, the reactive dissociations of these gaseous molecules would corrode or passivate the sliding surfaces, which cause an increase of adhesive force or a reduction of shear force, respectively. For dry inert gas, superlow friction is more feasible in N_2 than in Ar for the polymeric a-C:H:Si film, as indicated in Figure 15. This demonstrates that even a small diversity in molecular characteristic of surrounding gas can have a crucial influence on the frictional behaviors of a-C:H:Si film. The origin of superior antifriction performance in dry N_2 compared to that in dry Ar is not yet well understood. Some researchers have proposed that the formation of a perpendicularly oriented monolayer adsorbed on the contact interface by physical interactions between π-orbital of sp^2-C atoms and lone pair electrons of N_2 is probably the reason for superior friction-reduction behavior in dry N_2.[56] Hydrogen is well-known for its lubrication effect by saturation of any covalent dangling bonds exposed to the sliding interface. Friction between such H-passivated surfaces is expected to be low due to the produced electrostatic repulsive forces[8−11,28] or, recently proposed, the antibonding orbital interactions between different atoms at the sliding interface.[43] DFT calculations have predicted that a minimum partial pressure of H_2 at room temperature such as $P_H = 0.38$ Pa is required to passivate all the dangling bonds for diamond or diamond-like surfaces. Ultralow friction can be achieved with a fully H-passivated surface, by either increasing P_H or reducing the surrounding temperature T.[57] In spite of this, the present study indicates that not all the hydrogenated carbon films can achieve superlow friction even in a hydrogen-providing atmosphere such as diluent H_2 of 500 Pa, especially for the most hydrogen-deficient sp^2-bonded a-C:H:Si films (Figure 4). This demonstrates that the hydrogen coverage on the pristine film surface is also of critical importance for achieving superlubricity.[51] In humid air, the key mechanism for ultralow or superlow friction is surface passivation by gaseous species, especially water molecules. To form boundary lubrication, water molecules have to find some surface sites to reside. For a-C:H:Si films, the formation of a hydrophilic Si−OH layer (Figure 17) are expected to adsorb water molecules and thus provide sufficient water coverage on the contact surface. Recent ab initio MD simulation has directly observed that load-induced confinement is the driving force for diamond surface passivation by water dissociation. The Pauli repulsion between the fully saturated bonds, such as C−H and C−OH, can stand the applied load and prevent the facing surfaces from direct contact, which leads to a reduction of friction.[58] In corrosive O_2, the occurrence of adhesive bonds at the sliding interface activated by oxygen through releasing of hydrogen and oxidizing the film surface causes a noticeable friction increase. However, the friction in O_2 is still ultralow ($\mu_{ss} \sim 0.084$), which is most likely due to the low shear strength of this oxide layer and partly to the remaining passivation effect from some hydrocarbon radicals (Figure 17).

4.4. Synergistic Effect of Phase Transformation, Surface Passivation and Shear Localization. Phase transformation, especially the evolution of sp^3 to sp^2, has been frequently reported in a-C films based on the characterization of tribolayers by Raman, TEM and near edge X-Ray absorption fine structure (NEXAFS) spectroscopy.[24,26,27,29,49,59] Most simulation studies also depict an obvious sp^3-to-sp^2 rehybridization under shear deformation.[29,30,49−51,53] The formation of a graphitic carbon layer on the contact surface is generally speculated as the origin for friction reduction in a-C materials. However, no direct experimental observation has been provided to confirm this hypothesis. The produced sp^2 phase can exist either in clustered rings or in disordering units. Furthermore, from the steric point of view, it is also difficult to maintain a completely layered graphitic structure for a tribolayer with thickness of several hundred nanometers. Therefore, just simple rehybridization and amorphization cannot guarantee a superlow friction. Recent simulation results by Kunze et al.[29] and Ma et al.[30] propose that shear localization is more reasonable to account for the superlow friction in a-C films, due to high phase transformation and gradual ordering occurred in the tribolayer. It is emphasized that amorphous carbon does not undergo homogeneous Newtonian-fluid-like shear deformation throughout the material, but rather exhibit localized deformation in a very thin shear band. This speculation can find some experimental clue from the polymeric a-C:H:Si film when tribotested in dry N_2 (Figures 1a, 2a3 and 16a). The overall increase in the intensity of the Raman spectrum taken from the wear scar on ball surface indicates a remarkable increase in the sp^2-C fraction in the tribolayer. In addition, the enhanced D peak implies an abundance of sp^2-bonded rings. Due to the very thin thickness of this tribolayer (Figures 2a3 and 11a1), the most energetically favored pathway to achieve the recorded extremely low friction ($\mu_{ss} \sim 0.001$) is to be deeply ordered in the very thin localized

layer. In Ma's simulation,[30] this ordering process produced a layer-like shear band. Note that this layer-like sp^2 configuration is not of a perfect graphite structure but includes some distorted bonds and defects. However, a layered structure was not observed by Kunze[29] and his co-workers.[49] The morphology of this sp^2-rich tribolayer is still amorphous but orients its bonds mainly parallel to the sliding plane (smoothening effect). Correspondingly, a superlow friction regime ($\mu < 0.01$) was recorded by Ma whereas a relatively high friction coefficient ($\mu \sim 0.12$) was observed in the latter case.[49] On the basis of these results, the most likely scenario for the present polymeric a-C:H:Si film tribotested in dry N_2 is that the topmost sp^2-rich tribolayer possesses some degree of layering and simultaneously orient most of its covalent bonds parallel to the sliding direction. On the other hand, the plentiful hydrogen atoms inherent in the films stabilize the film structure and terminate the dangling bonds around the sliding interface (i.e., forming a GLCHH structure).[42] Therefore, the superlow friction for the polymeric a-C:H:Si film in dry N_2 is more likely attributed to the synergistic effect between phase transformation, shear localization and surface passivation. This synergistic effect is further interpreted in another MD simulation in which a self-mated H-rich (45%) a-C:H film undergoes a remarkable sp^3-to-sp^2 transformation in a region of ±1 nm around the sliding interface in the first 5 ns sliding at a pressure of 5 GPa. The film surfaces passivate themselves by hydrogen termination and orientation of sp^2-rings parallel to the sliding direction after about 20 ns, and the friction coefficient then drops to a low value for the rest 20 ns sliding.[50] In comparison, the superlubricity for the polymeric a-C:H:Si film in diluent H_2 is mainly ascribed to the passivation effect by hydrogen as discussed in Section 4.3, because no obvious ring-like structure is detected in the tribolayer (Figure 16b). The comparison between dry N_2 and H_2 implies that the degree of clustering of aromatic rings is favored with the increase of the chemical inertness of the surrounding gas. However, further work such as TEM observation is still needed to disclose the exact bonding structure of the produced tribolayers. In addition, how to avoid vast film material loss from the polymeric-film-coated ball in the running-in period when tribotested in dry N_2 or H_2 (i.e., Figures 2a3, 5a3 and 9) is also necessary, for providing more durable lubrication.

5. CONCLUSION

The origin of superlubricity in ion vapor deposited a-C:H:Si films has been investigated from a systematic standpoint. The results demonstrate that hydrogen-induced diversity in film structures such as polymer-like, diamond-like or sp^2-bonded a-C, and environmental gas characteristic are the two most influential factors controlling the frictional behaviors of a-C:H:Si films. A proper range of hydrogen content in the film is required to achieve stable superlow friction in a distinct gaseous atmosphere (i.e., dry N_2, reactive H_2 or humid air). The rapid buildup of tribolayers on the contact surfaces during running-in period is the key requirement for establishing superlubric state in dry N_2 and diluent H_2. Self-mated sliding is more effective in building up this antifriction tribolayer than that is slide against bare counterpart. Special attention has been given to the polymer-like a-C:H:Si (31.9 at. % H) film because this hydrogen-rich sample can exhibit superlow friction ($\mu \sim 0.001-0.01$) in various gaseous environments including humid air, inert gases (N_2 and Ar) and reactive gas (H_2), and can even maintain ultralow friction ($\mu \sim 0.084$) in a corrosive gas (O_2). Hydrogen is highlighted for its decisive role in obtaining superlow friction. The occurrence of superlubricity in a-C:H:Si films is sometimes attributed to a synergistic effect of phase transformation, surface passivation and shear localization, for example, the acquisition of an extremely low friction coefficient of ~0.001 in dry N_2. The contribution of each mechanism to the friction reduction depends on the specific tribotesting condition. The present realization of superlubricity by one material such as the polymer-like a-C:H:Si film in multi-environments may open up a new pathway for designing more efficient lubricating materials in the near future.

AUTHOR INFORMATION

Corresponding Author

*X. Chen. E-mail: chenxc1213@gmail.com. Tel./Fax: +81 358411631.

Notes

The authors declare no competing financial interest.

ACKNOWLEDGMENTS

We acknowledge Dr. M. Kawaguchi of Tokyo Metropolitan Industrial Technology Research Institute (TIRI) for his assistance in ToF-SIMS measurements. Special appreciation is given to Mr. S. Sawai and Mr. T. Itoh for their support in HRTEM observation. In addition, the authors are grateful to Dr. J. Choi for his valuable discussions.

REFERENCES

(1) Holmberg, K.; Andersson, P.; Erdemir, A. Global Energy Consumption due to Friction in Passenger Cars. *Tribol. Int.* **2012**, *47*, 221−234.

(2) Martin, J.-M. Superlubricity of Molybdenum Disulfide. In *Superlubricity*; Erdemir, A., Martin, J.-M., Eds.; Elsevier: Amsterdam, 2007; Chapter 13, pp 207−225.

(3) Hirano, M.; Shinjo, K. Atomistic Locking and Friction. *Phys. Rev. B* **1990**, *41*, 11837−11851.

(4) Müser, M. H. Structural Lubricity: Role of Dimension and Symmetry. *Europhys. Lett.* **2004**, *66*, 97−103.

(5) Hod, O. Interlayer Commensurability and Superlubricity in Rigid Layered Materials. *Phys. Rev. B* **2012**, *86*, 075444.

(6) Liu, Z.; Yang, J.; Grey, F.; Liu, J. Z.; Liu, Y.; Wang, Y.; Yang, Y.; Cheng, Y.; Zheng, Q. Observation of Microscale Superlubricity in Graphite. *Phys. Rev. Lett.* **2012**, *108*, 205503.

(7) Sankaran, K. J.; Kumar, N.; Kurian, J.; Ramadoss, R.; Chen, H.-C.; Dash, S.; Tyagi, A. K.; Lee, C.-Y.; Tai, N.-H.; Lin, I.-N. Improvement in Tribological Properties by Modification of Grain Boundary and Microstructure of Ultrananocrystalline Diamond Films. *ACS Appl. Mater. Interfaces* **2013**, *5*, 3614−3624.

(8) Donnet, C.; Fontaine, J.; Grill, A.; Le Mogne, T. The Role of Hydrogen on the Friction Mechanism of Diamond-like Carbon Films. *Tribol. Lett.* **2000**, *9*, 137−142.

(9) Erdemir, A.; Eryilmaz, O. L.; Nilufer, I. B.; Fenske, G. R. Effect of Source Gas Chemistry on Tribological Performance of Diamond-like Carbon Films. *Diamond Relat. Mater.* **2000**, *9*, 632−637.

(10) Erdemir, A.; Eryilmaz, O. L.; Fenske, G. R. Synthesis of Diamondlike Carbon Films with Superlow Friction and Wear Properties. *J. Vac. Sci. Technol., A* **2000**, *18*, 1987−1992.

(11) Erdemir, A.; Eryilmaz, O. L.; Nilufer, I. B.; Fenske, G. R. Synthesis of Superlow-Friction Carbon Films from Highly Hydrogenated Methane Plasmas. *Surf. Coat. Technol.* **2000**, *133−134*, 448−454.

(12) Konicek, A. R.; Grierson, D. S.; Gilbert, P. U. P. A.; Sawyer, W. G.; Sumant, A. V.; Carpick, R. W. Origin of Ultralow Friction and Wear in Ultrananocrystalline Diamond. *Phys. Rev. Lett.* **2008**, *100*, 235502.

(13) Cui, L.; Lu, Z.; Wang, L. Toward Low Friction in High Vacuum for Hydrogenated Diamondlike Carbon by Tailoring Sliding Interface. *ACS. Appl. Mater. Interfaces* **2013**, *5*, 5889−5893.
(14) Dienwiebel, M.; Verhoeven, G. S.; Pradeep, N.; Frenken, J. W. M.; Heimberg, J. A.; Zandbergen, H. W. Superlubricity of Graphite. *Phys. Rev. Lett.* **2004**, *92*, 126101.
(15) Kato, K.; Umehara, N.; Adachi, K. Friction, Wear and N_2-Lubrication of Carbon Nitride Coatings: A Review. *Wear* **2003**, *254*, 1062−1069.
(16) Martin, J.-M.; De Barros Bouchet, M.-I.; Matta, C.; Zhang, Q.; Goddard, W. A., III; Okuda, S.; Sagawa, T. Gas-Phase Lubrication of ta-C by Glycerol and Hydrogen Peroxide. Experimental and Computer Modeling. *J. Phys. Chem. C* **2010**, *114*, 5003−5011.
(17) Pei, Y. T.; Galvan, D.; De Hosson, J.; Th, M. Nanostructure and Properties of TiC/a-C:H Composite Coatings. *Acta Mater.* **2005**, *53*, 4505−4521.
(18) Sjöström, H.; Stafström, S.; Boman, M.; Sundgren, J.-E. Superhard and Elastic Carbon Nitride Thin Films Having Fullerenelike Microstructure. *Phys. Rev. Lett.* **1995**, *75*, 1336−1339.
(19) Liu, X.; Yang, J.; Hao, J.; Zheng, J.; Gong, Q.; Liu, W. A Near-Frictionless and Extremely Elastic Hydrogenated Amorphous Carbon Film with Self-Assembled Dual Nanostructure. *Adv. Mater.* **2012**, *24*, 4614−4617.
(20) Konicek, A. R.; Grierson, D. S.; Sumant, A. V.; Friedmann, T. A.; Sullivan, J. P.; Gilbert, P. U. P. A.; Sawyer, W. G.; Carpick, R. W. Influence of Surface Passivation on the Friction and Wear Behavior of Ultrananocrystalline Diamond and Tetrahedral Amorphous Carbon Thin Films. *Phys. Rev. B* **2012**, *85*, 155448.
(21) Kumar, N.; Ramadoss, R.; Kozakov, A. T.; Sankaran, K. J.; Dash, S.; Tyagi, A. K.; Tai, N. H.; Lin, I.-N. Humidity-Dependent Friction Mechanism in an Ultrananocrystalline Diamond Film. *J. Phys. D: Appl. Phys.* **2013**, *46*, 275501.
(22) Sankaran, K. J.; Kumar, N.; Chen, H.-C.; Dong, C.-L; Bahuguna, A.; Dash, S.; Kumar Tyagi, A.; Lee, C.-Y.; Tai, N.-H.; Lin, I.-N. Near Frictionless Behavior of Hydrogen Plasma Treated Diamond Nanowire Films. *Sci. Adv. Mater.* **2013**, *5*, 687−698.
(23) Radhika, R.; Kumar, N.; Sankaran, K. J.; Dumpala, R.; Dash, S.; Rao, M. S. R.; Arivuoli, D.; Tyagi, A. K.; Tai, N. H.; Lin, I.-N. Extremely High Wear Resistance and Ultra-Low Friction Behaviour of Oxygen-Plasma-Treated Nanocrystalline Diamond Films. *J. Phys. D Appl. Phys.* **2013**, *46*, 425304.
(24) Merkle, A. P.; Erdemir, A.; Eryilmaz, O. L.; Johnson, J. A.; Marks, L. D. In Situ TEM Studies of Tribo-Induced Bonding Modifications in Near-Frictionless Carbon Films. *Carbon* **2010**, *48*, 587−591.
(25) Pastewka, L.; Moser, S.; Gumbsch, P.; Moseler, M. Anisotropic Mechanical Amorphization Drives Wear in Diamond. *Nat. Mater.* **2011**, *10*, 34−38.
(26) Liu, Y.; Erdemir, A.; Meletis, E. I. An Investigation of the Relationship between Graphitization and Frictional Behavior of DLC Coatings. *Surf. Coat. Technol.* **1996**, *86*−*87*, 564−568.
(27) Sánchez-López, J. C.; Erdemir, A.; Donnet, C.; Rojas, T. C. Friction-Induced Structural Transformations of Diamondlike Carbon Coatings under Various Atmospheres. *Surf. Coat. Technol.* **2003**, *163*−*164*, 444−450.
(28) Erdemir, A. The Role of Hydrogen in Tribological Properties of Diamond-like Carbon Films. *Surf. Coat. Technol.* **2001**, *146*−*147*, 292−297.
(29) Kunze, T.; Posselt, M.; Gemming, S.; Seifert, G.; Konicek, A. R.; Carpick, R. W.; Pastewka, L.; Moseler, M. Wear, Plasticity, and Rehybridization in Tetrahedral Amorphous Carbon. *Tribol. Lett.* **2014**, *53*, 119−126.
(30) Ma, T.-B.; Wang, L.-F.; Hu, Y.-Z.; Li, X.; Wang, H. A Shear Localization Mechanism for Lubricity of Amorphous Carbon Materials. *Sci. Rep.* **2014**, *4*, 3662.
(31) Chen, X.; Kato, T.; Kawaguchi, M.; Nosaka, M.; Choi, J. Structural and Environmental Dependence of Superlow Friction in Ion Vapour-Deposited a-C:H:Si Films for Solid Lubrication Application. *J. Phys. D: Appl. Phys.* **2013**, *46*, 255304.
(32) Chen, X.; Kato, T. Growth Mechanism and Composition of Ultrasmooth a-C:H:Si Films Grown from Energetic Ions for Superlubricity. *J. Appl. Phys.* **2014**, *115*, 044908.
(33) Sha, Z.-D.; Sorkin, V.; Branicio, P. S.; Pei, Q.-X.; Zhang, Y.-W.; Srolovitz, D. J. Large-Scale Molecular Dynamics Simulations of Wear in Diamond-like Carbon at the Nanoscale. *Appl. Phys. Lett.* **2013**, *103*, 073118.
(34) Sugimoto, I.; Miyake, S. Oriented Hydrocarbons Transferred from a High Performance Lubricative Amorphous C:H:Si Film during Sliding in a Vacuum. *Appl. Phys. Lett.* **1990**, *56*, 1868.
(35) Asay, D. B.; Dugger, M. T.; Ohlhausen, J. A.; Kim, S. H. Macro- to Nanoscale Wear Prevention via Molecular Adsorption. *Langmuir* **2008**, *24*, 155.
(36) Barnette, A. L.; Asay, D. B.; Ohlhausen, J. A.; Dugger, M. T.; Kim, S. H. Tribochemical Polymerization of Adsorbed n-Pentanol on SiO_2 during Rubbing: When Does It Occur and Is It Responsible for Effective Vapor Phase Lubrication? *Langmuir* **2010**, *26*, 16299.
(37) Wang, P.; Hirose, M.; Suzuki, Y.; Adachi, K. Carbon Tribo-Layer for Super-Low Friction of Amorphous Carbon Nitride Coatings in Inert Gas Environments. *Surf. Coat. Technol.* **2013**, *221*, 163−172.
(38) Fontaine, J.; Le Mogne, T.; Loubet, J. L.; Belin, M. Achieving Superlow Friction with Hydrogenated Amorphous Carbon: Some Key Requirements. *Thin Solid Films* **2005**, *482*, 99−108.
(39) Beyer, W. Structural and Electrical Properties of Silicon-based Amorphous Alloys. *J. Non-Cryst. Solids* **1987**, *97*−*98*, 1027−1034.
(40) Chabal, Y. J.; Patel, C. K. N. Molecular Hydrogen in a-Si:H. *Rev. Mod. Phys.* **1987**, *59*, 835−844.
(41) Williamson, D. L.; Mahan, A. H.; Nelson, B. P.; Crandall, R. S. Microvoids in Amorphous $Si_{1-x}C_x$:H Alloys Studied by Small-Angle X-Ray Scattering. *Appl. Phys. Lett.* **1989**, *55*, 783−785.
(42) Casiraghi, C.; Ferrari, A. C.; Robertson, J. Raman Spectroscopy of Hydrogenated Amorphous Carbons. *Phys. Rev. B* **2005**, *72*, 085401.
(43) Bai, S.; Onodera, T.; Nagumo, R.; Miura, R.; Suzuki, A.; Tsuboi, H.; Hatakeyama, N.; Takaba, H.; Kubo, M.; Miyamoto, A. Friction Reduction Mechanism of Hydrogen- and Fluorine-Terminated Diamond-like Carbon Films Investigated by Molecular Dynamics and Quantum Chemical Calculation. *J. Phys. Chem. C* **2012**, *116*, 12559−12565.
(44) Dag, S.; Ciraci, S. Atomic Scale Study of Superlow Friction between Hydrogenated Diamond Surfaces. *Phys. Rev. B* **2004**, *70*, 241401.
(45) Zilibotti, G.; Righi, M. C.; Ferrario, M. Ab Initio Study on the Surface Chemistry and Nanotribological Properties of Passivated Diamond Surfaces. *Phys. Rev. B* **2009**, *79*, 075420.
(46) Robertson, J. Recombination and Photoluminescence Mechanism in Hydrogenated Amorphous Carbon. *Phys. Rev. B* **1996**, *53*, 16302−16305.
(47) Pokrovskii, V. N. The Mesoscopic Theory of the Slow Relaxation of Linear Macromolecules. *Adv. Polym. Sci.* **2001**, *154*, 143−219.
(48) Marino, M. J.; Hsiao, E.; Chen, Y.; Eryilmaz, O. L.; Erdemir, A.; Kim, S. H. Understanding Run-in Behavior of Diamond-like Carbon Friction and Preventing Diamond-like Carbon Wear in Humid Air. *Langmuir* **2011**, *27*, 12702−12708.
(49) Pastewka, L.; Moser, S.; Moseler, M.; Blug, B.; Meier, S.; Hollstein, T.; Gumbsch, P. The Running-in of Amorphous Hydrocarbon Tribocoatings: A Comparison between Experiment and Molecular Dynamics Simulations. *Int. J. Mater. Res.* **2008**, *99*, 1136−1143.
(50) Pastewka, L.; Moser, S.; Moseler, M. Atomistic Insights into the Running-in, Lubrication, and Failure of Hydrogenated Diamond-like Carbon Coatings. *Tribol. Lett.* **2010**, *39*, 49−61.
(51) Gao, G. T.; Mikulski, P. T.; Chateauneuf, G. M.; Harrison, J. A. The Effects of Film Structure and Surface Hydrogen on the Properties of Amorphous Carbon Films. *J. Phys. Chem. B* **2003**, *107*, 11082−11090.
(52) Schall, J. D.; Gao, G. T.; Harrison, J. A. Effects of Adhesion and Transfer Film Formation on the Tribology of Self-Mated DLC Contacts. *J. Phys. Chem. C* **2010**, *114*, 5321−5330.

(53) Gao, G. T.; Mikulski, P. T.; Harrison, J. A. Molecular-Scale Tribology of Amorphous Carbon Coatings: Effects of Film Thickness, Adhesion, and Long-Range Interactions. *J. Am. Chem. Soc.* **2002**, *124*, 7202−7209.
(54) Andersson, J.; Erck, R. A.; Erdemir, A. Friction of Diamond-like Carbon Films in Different Atmospheres. *Wear* **2003**, *254*, 1070−1075.
(55) Qi, Y.; Konca, E.; Alpas, A. T. Atmospheric Effects on the Adhesion and Friction between Non-Hydrogenated Diamond-like Carbon (DLC) Coating and Aluminum − A First Principles Investigation. *Surf. Sci.* **2006**, *600*, 2955−2965.
(56) Ji, L.; Li, H.; Zhao, F.; Quan, W.; Chen, J.; Zhou, H. Effects of Environmental Molecular Characteristics and Gas−Surface Interaction on Friction Behaviour of Diamond-like Carbon Films. *J. Phys. D Appl. Phys.* **2009**, *42*, 135301.
(57) Guo, H.; Qi, Y.; Li, X. Predicting the Hydrogen Pressure to Achieve Ultralow Friction at Diamond and Diamondlike Carbon Surfaces from First Principles. *Appl. Phys. Lett.* **2008**, *92*, 241921.
(58) Zilibotti, G.; Corni, S.; Righi, M. C. Load-Induced Confinement Activates Diamond Lubrication by Water. *Phys. Rev. Lett.* **2013**, *111*, 146101.
(59) Scharf, T. W.; Singer, I. L. Quantification of the Thickness of Carbon Transfer Films using Raman Tribometry. *Tribol. Lett.* **2003**, *14*, 137−145.